the increased gene expressions in the mice different from those used in the microarray experiments. In addition, an experiment with acute immobilization stress revealed that five of the seven genes exhibited a response to the stress in the neocortex of mice. After the five genes were characterized in an additional experiment using FG7142 and flumazenil, we discussed the mechanism of the stress-induced increase in the gene expression.

2. Material and methods

2.1. Animals and chemicals

The present animal experiments were performed in strict accordance with the guidelines of the Tokyo Medical and Dental University and were approved by the Animal Investigation Committee. Male C57BL mice (Japan Clea Laboratories, Japan) at postnatal ages of 8 weeks were used. The mice were kept at 22.0 ± 0.5 °C in a humidity-controlled room under a 12-h light–dark cycle (lights on at 8:00 a.m.) with free access to food and water. The animal experiments were conducted during the light cycle.

FG7142 (*N*-methyl-β-carboline-3-carboxamide) (TOCRIS, Bristol, UK) and flumazenil (ethyl-8-fluoro-5,6-dihydro-5-methyl-6-oxo-4H-imidazo [1,5-*a*][1,4]benzodiazepine-3-carboxylate) [a gift of the Astellas Pharamaceutical Company (Tokyo, Japan)] were dissolved in saline/40% 2-hydroxypropyl-β-cyclodextrin (Nacalai Tesque, Kyoto, Japan). FG7142 (20 mg/kg) was intraperitoneally injected in a volume of 5 mL/kg. The control animals received only the vehicle. Flumazenil (10 mg/5 mL/kg) was subcutaneously injected in the mice twice at 15 min before and 20 min after the injection of FG7142, taking into account the relatively short action of the drug. Consequently, the experiment consisted of four groups of animals, namely the vehicle + vehicle, vehicle + FG7142, flumazenil + vehicle and flumazenil + FG7142. No animals exhibited seizures in the behavioral monitoring throughout the experiments.

The acute immobilization stress of mice consisted of taping their limbs to a Plexiglas surface in the normal position for 1 h. Animals under the control condition remained in the home cage until their sacrifice.

Trunk blood was obtained from mice used in the stress experiments at the time of sacrifice. Serum obtained after centrifugation at 3500 rpm for 30 min was stored at −30 °C until the assay. Serum corticosterone was measured by radioimmunoassay (Corticosterone Double Antibody, [^{125}I] Ria Kit, MP Biomedicals, Inc., Irvine, CA, USA) with a highly specific corticosterone antiserum having a detection threshold of 7.7 ng/mL.

2.2. Extract of total RNA

The mice were killed by cervical dislocation 1 h later after the administration of FG7142 or after the immobilization stress for 1 h. The neocortex (the dorsal part of the cerebral cortex divided along the rhinal fissure) was rapidly removed in the cold, frozen in liquid nitrogen, and stored at −80 °C until use. Each frozen cortical tissue section was homogenized using a Polytron Homogenizer (Kinematica AG, Littau/Luzern, Switzerland) at 24,000 rpm for 10 s, and its total RNA was extracted using the Quiagen Rneasy Midi System (Quiagen, Valencia, CA, USA).

2.3. Microarray experiments

The RNA quality was examined by gel electrophoresis (Agilent Bioanalyzer). Twenty μg of pooled total RNA obtained from 9 or 10 animals was reverse transcribed using the oligo dT12-18 primer and aminoallyl-dUTP. The synthesized cDNA was labeled by a reaction with dye, NHS-ester Cy3 (the vehicle-treated sample) or NHS-ester Cy5 (the FG7142-treated sample) (Hughes et al., 2001). The labeled cDNA was applied to the DNA microarray (Mouse cDNA Microarray, Agilent) and was hybridized at 65 °C for 17 h. After washing, the microarray was scanned by a Microarray Scanner (ScanArray 5000, GSI Lumonics), and the image was analyzed using software (QuantArray, GSI Lumonics). The signal intensity of each spot was calibrated by subtraction of the intensity of the negative control and was normalized to the global value of all the genes provided on the membranes. Expression of a gene on a specific spot was considered as relevant if the signal intensity was greater than twice the SD of the background.

2.4. Quantitative RT-PCR

The RNA sample was obtained from a mouse different from that used in the microarray experiments. The sample was treated with RNase-free DNase I (Invitrogen, Carlsbad, CA, USA) to remove any contaminating genomic DNA. The single-stranded cDNA was then synthesized from 1 μg of the DNase I-treated neocortical RNA using a SuperScript Preamplification system (Invitrogen). The remaining RNAs were digested using Ribonuclease H (Invitrogen), and the resulting cDNA suspended in 10 volumes of TE buffer (10 mM Tris–HCl, pH 8.0, and 1 mM EDTA) was used for the quantitative RT-PCR analysis described below.

Five μL of a diluted sample of each first strand product was amplified using 2 μL of LightCycler FastStart DNA Master SYBER Green I (Roche Diagnostics, Mannheim, Germany) (Castello et al., 2002) and a pair of primers (Table 1) at the final concentration of 0.5 μM each and $MgCl_2$ at the final concentration of 3 mM. PCR was performed in a total volume of 20 μL for 10 min at 95 °C and 40 cycles of 15 s at 95 °C, 5 s at 65 °C and 10 s at 72 °C. The melting curve analysis was done by continuous acquisition from 65 to 95 °C with a temperature transition rate of 0.1 °C/s. In each assay, standard curves were generated from four increasing amounts of the pooled cDNA templates of equal volumes of the individual samples. The results were automatically calculated using the respective standard curves by the LightCycler analysis software version 3.5. Amplification of the single product in the RT-PCR was confirmed by monitoring the melting curve and by agarose gel electrophoresis. Expression of the glyceraldehyde-3-phosphate dehydrogenase (Gapdh) was determined as the internal standard

Table 1
Primer sequences for the semi-quantitative RT-PCR

Official symbol of gene	Gene Bank ID	Bases spanned	Forward primer (5′–3′)	Reverse primer (5′–3′)
Gapdh	NM_001001303	211–439	CGGCAAATTCAACGGCACAGTCAA	TGGGGGCATCGGCAGAAGG
Cyr61	NM_010516	630–858	CCCCCGGCTGGTGAAAGTC	ATGGGCGTGCAGAGGGTTGAAAAG
Fos	NM_010234	323–502	CCCACGGTGACAGCCATCTCCA	CTGCGCTCTGCCTCCTGACACG
Btg2	NM_007570	479–597	CCCCGGTGGCTGCCTCCTATG	GGGTCGGGTGGCTCCTATCTA
Adamts 1	NM_009621	550–896	GGCGCCCCACGGAGGAAG	AGGCGCTGGCTGAATGAAGAAC
Rgs 2	NM_009061	325–652	AGGGCGTTTTTAAAGTCCGAGTT	CCGTGGTGATCTGTGGCTTTTTAC
Gem	NM_010276	241–524	CTCCGAAACCGCCACTCTACTGCT	GTTCTCCCCCTTATTTTCCCACAT
Nr4a1	NM_010444	668–968	CTCCGCCACCTCCAACCTTCTTCT	GTGCGGACCCCATAGTGCTGACA

Table 2
The results of DNA microarray for the young adult mice

Gen Bank ID	Gene name	Official Symbol	Fold change
AA466852	Cysteine rich protein 61	Cyr61	4.17
AA002910	FBJ osteosarcoma oncogene	Fos	4.00
AA596779	B-cell translocation gene 2, anti-proliferative	Btg 2	3.31
AA711852	A disintegrin-like and metalloprotease with thrombospondin type 1	Adamts 1	2.94
AA221794	Regulator of G-protein signaling 2	Rgs 2	2.51
AA756727	GTP-binding protein (gene overexpressed in skeletal muscle)	Gem	2.39
AA209882	Nuclear receptor subfamily 4, group A, member 1	Nr4a1	2.16

Twenty μg of pooled total RNA obtained from 9 or 10 animals was used in each experiment of the DNA microarray. Fold changes were calculated by comparison between the FG7142-treated and the vehicle-treated levels.

for each sample, because the Gapdh gene has been reported to be a housekeeping gene that is constantly expressed in neural tissues (Thellin et al., 1999). The ratios of the results of the mRNAs of each gene to those of the Gapdh mRNAs were used for the statistical comparison as the normalized values of the mRNA of each gene.

2.5. Statistical analysis

The statistical analysis between the two groups (FG7142 and vehicle) were made using the two-tailed Student's *t*-test or Welch's *t*-test. In the experiment using both flumazenil and FG7142, the statistical differences were analyzed by a one-way analysis of variance (ANOVA) or Kruskal–Wallis analysis followed by Sheffe's multiple comparison test.

3. Results

Each significant gene regulated by the administration of FG7142 was selected according to the following criteria in the DNA microarray experiments. The signal intensity of a spot labeled with Cy3 (vehicle-treated sample) was greater than 500, and the calculated expression ratio of Cy5/Cy3 was greater than two or less than 0.5. The microarray experiment demonstrated that seven genes were significantly up-regulated in the neocortex of the 8-week-old mice (Table 2), while no significantly down-regulated gene was observed in the cortex. In animals different from those used in the microarray experiments, the seven genes were verified by the quantitative RT-PCR method, which demonstrated that treatment with FG7142 induced a significant increase in the mRNA of the seven genes in the cortex of the mice (Fig. 1).

The effects of immobilization stress on the seven genes by the RT-PCR method are shown in Fig. 2. There was a significant elevation in the cortical mRNA expression of five of the seven genes, i.e., Fos, Cyr61, Btg2, Adants1 and Gem, after the immobilization stress for 1 h.

The concentration of serum corticosterone (mean ± S.E.M., ng/mL) was significantly higher in the mice having undergone the immobilization stress (502 ± 22.8, $p < 0.001$, $n = 8$) than in the control mice (222 ± 22.4, $n = 10$).

We examined the effects of the co-administrations of flumazenil on the FG7142-induced increases in the mRNAs of the five genes in the neocortex of the mice (Fig. 3). Treatment with FG7142 failed to produce a statistically significant change in the cortical mRNA expression levels of all five genes in mice receiving the co-administrations of the benzodiazepine antagonist, while the administration of FG7142 induced a statistically significant increase in the mRNA levels of the genes in the mice injected with the vehicle of the antagonist. The expression levels of four genes, i.e., Cyr61, Fos, Btg2 and Gem, in the cortex of the mice treated with the vehicle of flumazenil and FG7142 were significantly higher than those of the mice receiving flumazenil and FG7142. In addition, there was no difference between the cortical levels of five genes of mice treated with the vehicle of flumazenil and the vehicle of FG7142 and those of mice treated with flumazenil and the vehicle of FG7142.

4. Discussion

The present study applied microarray technology to obtain an unprejudiced view of the effect of FG7142 on the neocortex of young adult mice. In the microarray experiment, the systemic

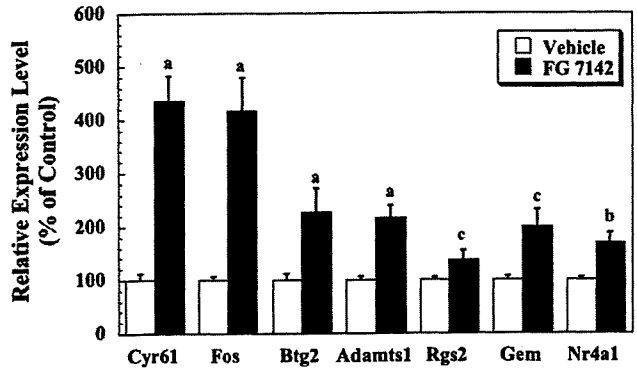

Fig. 1. Results of RT-PCR in the neocortex of mice after treatment with FG7142. FG7142 (20 mg/kg, i.p.) or the vehicle was injected into the mice. The mice were sacrificed at 1 h after the administration. Results are means with S.E.M. of data (normalized to Gapdh) obtained from seven or eight animals, and are expressed as a percentage of the mean value of the respective vehicle-treated mice. (a) $p < 0.001$, (b) $p < 0.01$ and (c) $p < 0.05$ compared to the vehicle-treated controls.

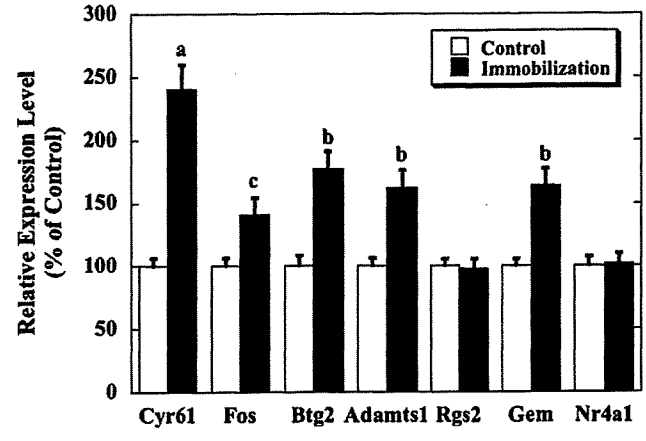

Fig. 2. Results of RT-PCR in the neocortex of mice after immobilization stress. The mice were sacrificed after the immobilization stress for 1 h. The control animals remained in the home cage until their sacrifice. Results are means with S.E.M. of data (normalized to Gapdh) obtained from 8 or 10 animals, and are expressed as a percentage of the mean value of the respective control mice. (a) $p < 0.001$, (b) $p < 0.01$ and (c) $p < 0.05$ compared to the controls.

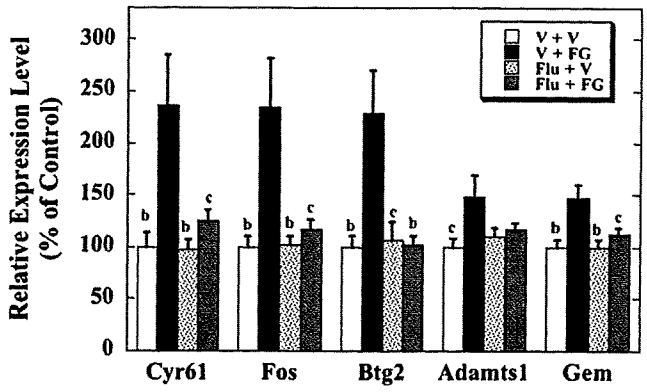

Fig. 3. Results of RT-PCR in the neocortex of mice after treatment with flumazenil and FG7142. FG7142 (20 mg/kg) or the vehicle was intraperitoneally injected into the mice 1 h before their sacrifice. Flumazenil (10 mg/kg) or the vehicle was subcutaneously injected into the mice twice, at 15 min before and 20 min after the administration of FG7142 or the vehicle. Thus, the experiment consisted of four groups of animals, namely the vehicle + vehicle (V + V), vehicle + FG7142 (V + FG), flumazenil + vehicle (Flu + V) and flumazenil + FG7142 (Flu + FG). Results are means with S.E.M. of data (normalized to Gapdh) obtained from seven or eight animals, and are expressed as a percentage of the mean value of the respective vehicle and vehicle-treated mice (V + V). The statistical differences were analyzed by a one-way analysis of variance (ANOVA) or Kruskal–Wallis analysis followed by Sheffe's multiple comparison test. (a) $p < 0.001$ vs. vehicle + FG7142, (b) $p < 0.01$ vs. vehicle + FG7142 and (c) $p < 0.05$ vs. vehicle + FG7142.

administration of FG7142 produced increased expressions of seven genes in the cortex. The RT-PCR experiment verified an enhanced expression of the mRNA of all seven genes in the brain area after the administration of the drug. In addition, the present study also demonstrated an outstanding result in which five of the seven genes including Fos were similarly activated in the molecular response to the immobilization stress in the neocortex of the mice, suggesting that the activated genes are involved in the stress-responsive molecular system.

FG7142 acts at the benzodiazepine sites of the $GABA_A$ receptors as a partial inverse agonist (Braestrup et al., 1984; Atack et al., 2005). Indeed, co-administrations of flumazenil, an antagonist at the benzodiazepine binding site, indicated that the effects of FG7142 on stress-related gene expression in the neocortex may be mediated via action of FG7142 at the benzodiazepine binding site of the $GABA_A$ receptors, because the injection of FG7142 failed to produce a significant increase in the cortical mRNAs in mice receiving the co-administrations of flumazenil.

Both FG7142 and stress, e.g., foot-shock and restraint stress similarly produce an immediate and transient (from 20 to 100 min) increased release of dopamine (Bradberry et al., 1991; Dazzi et al., 2003, 2004), noradrenaline (Nakane et al., 1994), and glutamate (Moghaddam, 1991; Karreman and Moghaddam, 1996) in the cerebral cortex of rodents. The increased release of monoamines (Bradberry et al., 1991; Nakane et al., 1994) and glutamate (Karreman and Moghaddam, 1996) after treatment with FG7142 is also blocked by the benzodiazepines. In addition, a deficit in the prefrontal cortical cognitive function induced by FG7142 is inhibited by a dopamine receptor antagonist (Murphy et al., 1996a,b) as well as by an adrenergic receptor antagonist (Birnbaum et al., 1999). Although the mechanism whereby FG7142 and immobilization stress similarly produced the increased expression of the stress-responsive genes in the present study is still unclear, it is likely that the activation of monoaminergic and/or glutamatergic neurons may be linked to the enhanced gene expression.

We have previously reported that the systemic injection of 20 mg/kg of FG7142 induced an increased Fos-like immunoreactivity in some brain areas of rats including the neocortex (Kurumaji et al., 2003). It has been established that there is an immediate up-regulation of the cortical expression of Fos after various stressors, such as the immobilization stress (Senba and Ueyama, 1997; Kovács, 1998). The present study also demonstrated that the enhanced gene expression of Fos in the neocortex of mice was induced 1 h after the pharmacological stressor as well as after the immobilization stress.

It has been reported that the other stress-responsive genes demonstrated by the present study, i.e., Cyr61, Adamts1 and Btg2 were increased in the states and models of neurodegenerative disorders. Cyr61 is a member of the CCN family of secreted matricellular proteins that bridge the functional and physical gap between the extracellular matrix-associated proteins and cell surface molecules (Perbal, 2004; Chaqour and Goppelt-Struebe, 2006). An increased Cyr61 expression was induced by a transient ischemic stroke (Schwarz et al., 2002). Adamts1 is the first member of ADAMTS (a disintegrin and metalloprotease with thrombospondin motifs) (Kuno et al., 1997) and has been shown to display anti-angiogenic properties (Vázquez et al., 1999). The gene expression of Adamts1 has increased during a physical or toxic injury (Sasaki et al., 2001; Cross et al., 2006) and in neurological diseases, such as Alzheimer's disease and Parkinson disease (Miguel et al., 2005). Btg2 is a member of the PC3/BTG/TOB family (Tirone, 2001). The potential roles of Btg2 have been suggested to be a transcriptional co-regulator, and differentiation and anti-apoptotic factor in neurogenesis (Iacopetti et al., 1999; Lim, 2006). The Btg2 gene expression was induced in response to the neurotoxin, domoic acid (Ryan et al., 2005) and seizure (Jung et al., 1996; Flood et al., 2004) in the brain of rodents. It appears that the changed gene expressions associated with the states and models of neurodegenerative disorders may be a sensitive molecular response to the pathological circumstances of the brain areas.

It has been established that Gem belongs to a superfamily of small GTP-binding proteins which behave as molecular signal transducers by interacting with calmodulin (Béguin et al., 2001; Maguire et al., 1994).

In conclusion, the pharmacological stressor produced an increased gene expression in the seven genes in the neocortex of mice. Five of the seven genes were similarly involved in the molecular response to the immobilization stress in the brain area, which have a variety of physiological functions in extracellular matrices as well as in the signal transduction system in the CNS. The genes can be regarded as candidate genes that play a role in the stress-response. As stress has been applied as a model to investigate the pathophysiology of the psychiatric disorders (Moghaddam, 2002; Duman and Monteggia, 2006), further studies to clarify the molecular cascade of the stress-responsive genes including other brain areas, such as the hippocampus and amygdala may provide a new avenue to important investigations.

Acknowledgements

This work was partly supported by research grants from the Ministry of Health, Labor and Welfare (Japan), and a Grant-in-Aid for Scientific Research from the Ministry of Education, Science, Culture and Sports (Japan).

References

Atack, J.R., Hutson, P.H., Collinson, N., Marshall, G., Bently, G., Moyes, C., Cook, S.M., Collins, I., Wafford, K., McKernan, R.M., Dawson, G.R., 2005. Anxiogenic properties of an inverse agonist selective for α3 subunit-containing $GABA_A$ receptors. Br. J. Pharmacol. 144, 357–366.

Béguin, P., Nagashima, K., Gonoi, T., Shibasaki, T., Takahashi, K., Kashima, Y., Ozaki, N., Geering, K., Iwanaga, T., Seino, S., 2001. Regulation of Ca^{2+} channel expression at the cell surface by the small G-protein kir/gem. Nature 411, 701–706.

Birnbaum, S.G., Gobeske, K.T., Auerbach, J., Taylor, J.R., Amsten, A.F.T., 1999. A role for norepinephrine in stress-induced cognitive deficits: alpha-1-adrenoceptor mediation in the prefrontal cortex. Biol. Psychiatry 46, 1266–1274.

Birnbaum, S.G., Yuan, P.X., Wang, M., Vijayraghavan, S., Bloom, A.K., Davis, D.J., Gobeske, K.T., Sweatt, J.D., Manji, H.K., Arnsten, A.F.T., 2004. Protein kinase C overactivity impairs prefrontal cortical regulation of working memory. Science 306, 882–884.

Bradberry, C.W., Lory, J.D., Roth, R.H., 1991. The anxiogenic beta-carboline FG7142 selectively increases dopamine release in rat prefrontal cortex as measured by microdialysis. J. Neurochem. 56, 748–752.

Braestrup, C., Honoré, T., Nielsen, M., Petersen, E.N., Jensen, L.H., 1984. Ligands for benzodiazepine receptor with positive and negative efficacy. Biochem. Pharmacol. 33, 859–862.

Castello, R., Estelles, A., Vazquez, C., Falco, C., Espana, F., Almenar, S.M., Fuster, C., Aznar, J., 2002. Quantitative real-time reverse transcription-PCR assay for urokinase plasminogen activator, plasminogen activator inhibitor type 1, and tissue metalloproteinase inhibitor type 1 gene expressions in primary breast cancer. Clin. Chem. 48, 1288–1295.

Chaqour, B., Goppelt-Struebe, M., 2006. Mechanical regulation of the Cyr61/CCN1 and CTGF/CCN2 proteins; implications in mechanical stress-associated pathologies. FEBS J. 273, 3639–3649.

Cross, A.K., Haddock, G., Stock, C.J., Allan, S., Surr, J., Bunning, R.A.D., Buttle, D.J., Woodroofe, M.N., 2006. ADAMTS-1 and -4 are up-regulated following transient middle cerebral artery occlusion in the rat and their expression is modulated by TNF in cultured astrocytes. Brain Res. 1088, 19–30.

Dazzi, L., Seu, E., Cherchi, G., Biggio, G., 2003. Antagonism of the stress-induced increases in cortical norepinephrine output by the selective norepinephrine reuptake inhibitor reboxetine. Eur. J. Pharmacol. 476, 55–61.

Dazzi, L., Seu, E., Cherchi, G., Biggio, G., 2004. Inhibition of stress-induced dopamine output in the rat prefrontal cortex by chronic treatment with olanzapine. Biol. Psychiatry 55, 477–483.

Dorow, R., Horowski, R., Paschelke, G., Amin, M., Braestrup, C., 1983. Severe anxiety induced by FG7142, a Beta-carboline ligand for benzdiazepine receptors. Lancet I (8), 98–99.

Duman, R.S, Monteggia, L.M., 2006. A neurotrophic model for stress-related mood disorders. Biol. Psychiatry 59, 1116–1127.

Ellicott, A., Hammen, C., Gitlin, M., Brown, G., Jamison, K., 1990. Life events and course of bipolar disorder. Am. J. Psychiatry 147, 1194–1198.

Evans, A.K., Lowry, C.A., 2007. Pharmacology of the β-carboline FG7142, a partial inverse agonist at the benzodiazepine allosteric site of the $GABA_A$ receptor: neurochemical, neurophysiological, and behavioral effects. CNS Drug Rev. 13, 475–501.

Flood, W.D., Moyer, R.W., Tsykin, A., Sutherland, G.R., Koblar, S.A., 2004. Nxf and Fbxo33: novel seizure-responsive genes in mice. Eur. J. Neurosci. 20, 1819–1826.

Hughes, T., Mao, M., Jones, A.R., Burchard, J., Marton, M.J., Shannon, K.W., Lefkowitz, S.M., Ziman, M., Schelter, J.M., Meyer, M.R., Kobayashi, S., Davis, C., Dai, H., He, Y.D., Stephaniants, S.B., Cavet, G., Walker, W.L., West, A., Coffey, E., Shoemaker, D.D., Stoughton, R., Blanchard, A.P., Friend, S.H., Linsley, P.S., 2001. Expression profiling using microarrays fabricated by an ink-jet oligonucleotide synthesizer. Nat. Biotechnol. 19, 342–347.

Iacopetti, P., Michelini, M., Stuckmann, I., Oback, B., Aaku-Saraste, E., Huttner, W.B., 1999. Expression of the antiproliferative gene TIS21 at the onset of neurogenesis identifies signal neuroepithelial cells that switch from proliferative to neuron-generating division. Proc. Natl. Acad. Sci. U.S.A. 96, 4639–4644.

Jung, H.Y., Kang, U.G., Ahn, Y.M., Joo, Y.H., Joo-Bae, P., Kim, Y.S., 1996. Induction of tetradecanoyl phorbol acetate-inducible sequence (TIS) genes by electroconvulsive shock in rat brain. Biol. Psychiatry 40, 503–507.

Karreman, M., Moghaddam, B., 1996. Effects of a pharmacological stressor on glutamate efflux in the prefrontal cortex. Brain Res. 716, 180–182.

Kendler, K.S., Karkowski, L.M., Prescott, C.A., 1999. Causal relationship between stressful events and the onset of major depression. Am. J. Psychiatry 156, 837–841.

Kovács, K.J., 1998. c-Fos as a transcription factor: a stressful (re)view from a functional map. Neurochem. Int. 33, 287–297.

Kuno, K., Kanada, N., Nakajima, E., Fujiki, F., Ichimura, F., Matsushima, K., 1997. Molecular cloning of a gene encoding a new type of metalloproteinase-disintegrin family protein with thombospondin motifs as an inflammation associated gene. J. Biol. Chem. 272, 556–562.

Kurumaji, A., Umino, A., Tanami, A., Ito, A., Asakawa, M., Nshikawa, T., 2003. Distribution of anxiogenic-induced c-fos in the forebrain regions of developing rats. J. Neural Transm. 110, 1161–1168.

Lim, I.K., 2006. TIS21/BTG2/PC3 as a link between aging and cancer; cell cycle regulator and endogenous cell death molecule. J. Cancer Res. Clin. Oncol. 132, 417–426.

Maguire, J., Santoro, T., Jensen, P., Siebenlist, U., Yewdell, J., Kelly, K., 1994. Gem—an induced, immediate-early protein belonging to the Ras family. Science 265, 241–244.

Miguel, R.F., Pollak, A., Lubec, G., 2005. Metalloproteinase ADAMTS-1 but not ADAMTS-5 is manifold overexpressed in neurodegenerative disorders as Down syndrome, Alzheimer's and Pick's disease. Mol. Brain Res. 133, 1–5.

Mikkelsen, J.D., Søderman, A., Kiss, A., Mirza, N., 2005. Effects of benzodizepines receptor agonists on the hypothalamic–pituitary–adrenocortical axis. Eur. J. Pharmacol. 519, 223–230.

Moghaddam, B., 1991. Stress preferentially increases extraneuronal levels of excitatory amino acids in the prefrontal cortex: comparison to hippocampus and basal ganglia. J. Neurochem. 60, 1650–1657.

Moghaddam, B., 2002. Stress activation of glutamate neurotransmission in the prefrontal cortex: implication for dopamine-associated psychiatric disorders. Biol. Psychiatry 51, 775–787.

Murphy, B.L., Arnsten, A.F.T., Goldman-Rakic, P.S., Roth, R.H., 1996a. Increased dopamine turnover in the prefrontal cortex impairs spatial working memory performance in rats and monkeys. Proc. Natl. Acad. Sci. U.S.A. 93, 1325–1329.

Murphy, B.L., Arnsten, A.F.T., Jentsch, J.D., Roth, R.H., 1996b. Dopamine and spatial working memory in rats and monkeys: pharmacological reversal of stress-induced impairment. J. Neurosci. 16, 7768–7775.

Nakane, H., Shimizu, N., Hori, T., 1994. Stress-induced norepinephrine release in the rat prefrontal cortex measured by microdialysis. Am. J. Physiol. 267, R1559–R1566.

Norman, R.M., Malla, A.K., 1993. Stressful life events and schizophrenia. I: a review of the research. Br. J. Psychiatry 162, 161–166.

Pellow, A., File, S.E., 1985. The effects of putative anxiogenic compound (FG7142.CGS 8216 and RO 15-1788) on the rat corticosterone response. Physiol. Behav. 35, 587–590.

Pellow, S., File, S.E., 1986. Anxiolytic and anxiogeic drug effects on exploratory activity in an elevated plus-maze: a novel test of anxiety in the rat. Pharmacol. Biochem. Behav. 24, 525–529.

Perbal, B., 2004. CCN proteins: multifunctional signaling regulators. Lancet 363, 62–64.

Ryan, J.C., Morey, J.S., Ramsdell, J.S., Dolah, M.V., 2005. Acute phase gene expression in mice exposed to the marine neurotoxin domoic acid. Neuroscience 136, 1121–1132.

Rodgers, R.J., Cole, J.C., Aboualfa, K., Stephenson, L.H., 1995. Ethopharmacological analysis of the effects of putative 'anxiogenic' agents in the mouse. Pharmacol. Biochem. Behav. 52, 805–813.

Sasaki, M., Seo-Kiryu, S., Kato, R., Kita, S., Kiyama, H., 2001. A disintegrin and metalloproetase with thrombospondin type1 motifs (ADAMTS-1) and IL-1 receptor type 1 mRNAs are simultaneously induced in nerve injured motor neurons. Mol. Brain Res. 89, 158–163.

Schwarz, D.A., Barry, G., Mackay, K.B., Manu, F., Naeve, G.S., Vana, A.M., 2002. Identification of differentially expressed genes induced by transient ischemic stroke. Mol. Brain Res. 101, 12–22.

Senba, E., Ueyama, T., 1997. Stress-induced expression of immediate early gene in the brain and peripheral organs of the rat. Neurosci. Res. 29, 183–207.

Singewald, N., Salchner, P., Sharp, T., 2003. Induction of c-fos expression in specific areas of the fear circuitry in rat forebrain by anxiogenic drugs. Biol. Psychiatry 53, 275–283.

Takamatsu, H., Noda, A., Kurumaji, A., Murakami, Y., Tatsumi, M., Ichise, R., Nishimura, S., 2003. A PET study following treatment with a pharmacological stressor, FG7142, in conscious rhesus monkeys. Brain Res. 980, 275–280.

Tam, S.Y., Roth, R.H., 1990. Modulation of mesocortical dopamine neurons by central benzodiazepine receptors. I. Pharmacological characterization. J. Pharmacol. Exp. Ther. 252, 989–996.

Thellin, O., Zorzi, W., Lakaye, B., De Borman, B., Coumans, B., Hennen, G., Grisar, T., Igout, A., Heinen, E., 1999. Housekeeping genes as internal standards: use and limits. J. Biotechnol. 75, 291–295.

Tirone, F., 2001. The gene PC3TIS21/BTG2, prototype member of the PC3/BTG/TOB family: regulator in control of cell growth, differentiation, and DNA repair. J. Cell Physiol. 187, 155–165.

Vázquez, F., Hastings, G., Ortega, M.-A., Lane, T.F., Oikemus, S., Lombardo, M., Iruela-Arispe, M.L., 1999. METH-1, a human ortholog of ADAMTS-1, and METH-2 are members of a new family of proteins with angio-inhibitory activity. J. Biol. Chem. 274, 23349–23357.

International Journal of Neuropsychopharmacology (2009), **12**, 1–16. Copyright © 2009 CINP
doi:10.1017/S1461145709009997

ARTICLE

CINP

Developmentally regulated and thalamus-selective induction of *leiomodin2* gene by a schizophrenomimetic, phencyclidine, in the rat

Hironao Takebayashi, Naoki Yamamoto, Asami Umino and Toru Nishikawa

Section of Psychiatry and Behavioral Sciences, Tokyo Medical and Dental University Graduate School, Tokyo, Japan

Abstract

The onset of schizophrenia and the schizophrenomimetic effects of an *N*-methyl-D-aspartate (NMDA) receptor antagonist, ketamine, rarely occur during infancy and childhood, suggesting that schizophrenia-related neuron circuits and molecules in the brain might show an age-related response to an NMDA receptor antagonist. By using a DNA microarray technique, we have identified the developmentally regulated PCP-inducible gene *leiomodin2* (*Lmod2*) that encodes a tropomyosin-binding actin-capping protein enriched in the cardiac and skeletal muscles. PCP caused an increase in the thalamic amounts of *Lmod2* transcripts at postnatal days (PD) 32 and 50 without affecting them at PD 8, 13, 20 and 24, while the NMDA antagonist failed to produce a significant change in the gene expression in the adult heart. *In-situ* hybridization analysis revealed that the basal and PCP-induced expression of the *Lmod2* gene is almost confined to the lateral and anterior nuclei of the thalamus among the brain regions at PD 50. The PCP-induced up-regulation of *Lmod2* mRNAs in the adult thalamus was mimicked totally (also up-regulated) by another NMDA antagonist, dizocilpine, and partly by the indirect dopamine agonist, methamphetamine. Moreover, pretreatment with a D_2-preferring dopamine receptor antagonist, haloperidol, partially antagonizes the increasing effects of PCP on thalamic *Lmod2* gene expression. These findings suggest that *Lmod2* might be involved in the pathophysiology of the age-dependent onset of drug-induced schizophrenia-like psychosis and schizophrenia and that the limited thalamic nuclei expressing the *Lmod2* gene could compose the neuron circuits that are specifically disturbed in these mental disorders.

Received 19 August 2008; Reviewed 17 September 2008; Revised 5 January 2009; Accepted 9 January 2009

Key words: *Leiomodin2* gene (*Lmod2*), phencyclidine, postnatal development, schizophrenia, thalamus.

Introduction

Schizophrenia is a serious brain disorder that exhibits high prevalence, frequent onset during youth, and a wide variety of mental dysfunctions including numerous refractory symptoms and often deprives patients of a complete re-entry into society (Buchanan & Carpenter, 2005). To understand the pathophysiology of this complex disorder, the psychotic state induced by phencyclidine [1(1-phenylcyclohexyl)-piperidine; PCP] and other antagonists for the *N*-methyl-D-aspartate (NMDA)-type glutamate receptor has been considered as a most useful pharmacological model for schizophrenia because (1) these drugs produce positive and negative symptoms and cognitive disturbances which are indistinguishable from those of schizophrenia from the cross-sectional view while the longitudinal progressions of NMDA antagonist-induced psychosis and schizophrenia are different (Javitt & Zukin, 1991); (2) a group of schizophrenia patients suffered exacerbation of their psychotic symptoms with a challenge dose of PCP and a chemically PCP-related and non-competitive antagonist for the NMDA receptor, ketamine (Javitt & Zukin, 1991; Lahti *et al.* 2001; Petersen & Stillman, 1978), and (3) the psychotomimetic effects of the ketamine stereoisomers are closely correlated with their affinities for the NMDA receptor (Gouzoulis-Mayfrank *et al.* 2005; Vollenweider *et al.* 1997).

Address for correspondence: Dr T. Nishikawa, Section of Psychiatry and Behavioral Sciences, Tokyo Medical and Dental University Graduate School, 1-5-45 Yushima, Bunkyo-ku, Tokyo 113-8519, Japan.
Tel.: #81-3-5803-5237 *Fax*: #81-3-5803-0135
Email: tnis.psyc@tmd.ac.jp

These schizophrenomimetic actions may be explained by the possibility that NMDA antagonists disturb the molecular and cellular equipment in an information-processing system or neuron circuit that specifically malfunctions in schizophrenia (Ito *et al.* 2007; Sato *et al.* 1997). Although the exact causative mechanism for schizophrenia remains unclear, the pathophysiological changes in the information-processing system might be associated with the development-dependent nature of schizophrenia and NMDA antagonist-induced psychosis (Ito *et al.* 2007; Sato *et al.* 1997). Thus, the onset of schizophrenia typically occurs after adolescence (Buchanan & Carpenter, 2005). It has been consistently reported that PCP-induced clinical symptoms and signs are mostly neurological in infants and young children but mainly psychiatric in adults; however, PCP has been observed to produce some psychiatric symptoms in young people (Schwartz & Einhorn, 1986; Welch & Correa, 1980). Ketamine has been observed to often produce psychotic symptoms in adults, but not in children (Reich & Silvay, 1989; White *et al.* 1982). In experimental animals, the behavioural effects of NMDA receptor antagonists have also been observed to alter during postnatal development. For instance, PCP (1 ~ 4 mg/kg) and dizocilpine (MK-801; 0.1 ~ 0.4 mg/kg) produced different dose–effect curves and peak activity levels in inducing hyperactivity between postnatal days (PD) 12 and 19 (Scalzo & Burge, 1994). Repeated treatment with PCP from PD 22–30, but not from PD 1–9, augments the ability of a subsequent challenge of the NMDA antagonist to elicit abnormal behaviour (Scalzo & Holson, 1992), which is thought to be an animal model for the hypersensitivity of schizophrenia patients to PCP and ketamine.

The late-developing features of schizophrenia and its pharmacological models indicate that maturation of the specific neuronal systems could be required for their onset. We can therefore postulate that the schizophrenia-related information-processing system might mature around adolescence in humans or a critical period of the postnatal development in experimental animals and could not play a crucial role in the regulation of mental functions or behaviour before these climactic periods. The hypothetical human system and its animal homolog should contain molecules that are responsive to NMDA antagonists only after adolescence and the critical period for the animal model of schizophrenia.

The plausible maturation process appears to be reflected in our observations that the distribution of brain c-Fos expression, which has long been used as a marker for changes in various brain cellular activities including metabolic and neural signal pathways (Morgan & Curran, 1991) following PCP administration, altered markedly during postnatal development (Nishikawa *et al.* 1998; Sato *et al.* 1997). Indeed, we recently found that acute systemic administration of PCP produced marked and insignificant alterations, respectively, of connective tissue growth factor/cysteine-rich 61/nephroblastoma overexpressed [*CCN1* = cysteine-rich protein 61 (*CYR61*)] mRNA expression in the neocortex of rats aged 56 d and 8 d (Ito *et al.* 2007). To further explore candidates for schizophrenia-linked and developmentally regulated molecules, we compared the effects of PCP on gene expression in the thalamus between the infant and young adult periods in rats using a DNA microarray and the RT–PCR technique.

The thalamus was selected for the screening experiments because (1) not only the neocortex (Sato *et al.* 1997) but also the thalamus (Nishikawa *et al.* 1998) exhibits the prominent postnatal changes in PCP-induced abnormal activities as revealed by c-*fos* gene expression before and after the critical period, (2) schizophrenia patients have been reported to show neurochemical, neuropathological, neurophysiological and *in-vivo* imaging abnormalities in or closely associated with the thalamus (Andreasen *et al.* 1977; Clinton & Meador-Woodruff, 2004; Sim *et al.* 2006), and (3) EEG, neuroimaging and brain activity mapping studies have suggested that the thalamus is one of the essential sites of action of NMDA antagonists in humans (Greifenstein *et al.* 1958; Vollenweider *et al.* 1997; Watis *et al.* 2008) and experimental animals (Dragunow & Faull, 1990; Duncan *et al.* 1999; Miyasaka & Domino, 1968).

Materials and methods

Animals

The animal experiments were performed in strict accordance with the guidelines of the Tokyo Medical and Dental University and were approved by the Committee for Animal Experiment Ethics of the University. Male Wistar rats (ST strain, Clea Japan, Japan) at PD 8 (15–25 g), PD 13 (20–30 g), PD 20 (35–45 g), PD 26 (60–80 g), PD 32 (100–120 g), and PD 50 (200–260 g) were used. The animals were housed at 24.0 ± 0.5 °C under a 12-h light/dark cycle (lights on 00:00 hours) and had free access to food and water. In our experiments we used only male rats to study the effects of PCP because onset of the menstrual cycle in females has been suggested to modify behavioural and biochemical responses to a variety of drugs.

Chemicals

PCP hydrochloride was kindly synthesized and donated by Astellas Pharma Inc. (Japan). Methamphetamine (MAP) hydrochloride was purchased from Dainippon Sumitomo Pharma Co., Ltd (Japan) with official permission of the Tokyo Metropolitan Bureau of Public Health. The other chemicals used were of ultrapure quality and were commercially available. PCP hydrochloride, MAP hydrochloride and dizocilpine hydrogen maleate (MK-801 hydrogen maleate; [5R,10S]-[+]-5-methyl-10,11-dihydro-5Hdibenzo[a,d] cyclohepten-5,10-imine) were dissolved in saline for subcutaneous (s.c.) injection. Haloperidol (Hal) was dissolved in 0.15% tartaric acid and titrated with 0.05 M NaOH to ~pH 5.0. Some animals were pretreated with Hal injection intraperitoneally (i.p.) 30 min before PCP (Sakurai *et al.* 2004). Control animals received the same volume of saline or vehicle. The doses of these drugs always refer to the free bases and were chosen in order to cause robust and typical behavioural and biochemical effects (Sakurai *et al.* 2004; Shintomi, 1975; Shirayama *et al.* 2000).

Behavioural ratings

On each day of the experiment, rats were placed individually into plastic observation cages (internal dimensions: 37 cm × 22 cm × 14 cm), allowed at least 90 min to habituate to the new environment, and were monitored for stereotypy, which is considered to be a model for schizophrenia symptomatology according to the PCP behaviour rating scales (Sturgeon *et al.* 1979), with minor modifications as described previously (Tanii *et al.* 1994) (see Fig. 2*b* legend). Behavioural ratings were made every 10 min from 30 to 60 min after acute PCP injection. The cumulative behavioural rating for each animal was determined as the summation of every 10-min score for the last 30 min.

Tissue and total RNA preparation

Rats were killed by cervical dislocation 60 or 90 min after administration of various drugs or saline. The thalamus, other discrete brain regions and the heart were rapidly dissected out in the cold, frozen in liquid nitrogen, and stored at −80 °C until required. The total RNA was prepared from these frozen rat tissues using an RNeasy Midi kit (Qiagen GmbH, Germany). The RNA quality was verified by gel electrophoresis (Agilent Bioanalyzer, USA).

DNA microarray

We performed DNA microarray analysis using the Affymetrix Rat Genome 230 2.0 arrays (Affymetrix, USA) to isolate the developmentally regulated transcripts responsive to PCP in the thalamus. These arrays contained 31 000 probe sets capable of analysing the expression level of over 30 000 transcripts and variants from over 28 000 well-substantiated rat genes. Further details can be obtained at http://www.affymetrix.com.

For this screening step, the following four experimental groups of rats were prepared: five saline-injected control rats at PD 50; five PCP (7.5 mg/kg s.c.)-treated rats at PD 50; five saline-injected control rats at PD 8; five PCP (7.5 mg/kg s.c.)-treated rats at PD 8. Equal amounts of total RNA individually isolated from the five animals of each experimental group were pooled in each experimental group. cDNA synthesis, cRNA labelling, hybridization and scanning were done according to the manifacturer's instructions (Affymetrix) (see Table 2 note). This first screening step to search for the candidate genes was accomplished by a single microarray comparison on the four pooled cDNAs from the respective four experimental groups. The 3′:5′ ratios of GAPDH, hexokinase, and β-actin of all four samples used were less than 1.2, 2.2, and 3.0, respectively, and thus satisfied the sample quality standard indicated as the signal value ratio <3. The excellent inter- and intra-platform reproducibility of the Affymetrix microarray (more than 88% and 90%, respectively) have been reported elsewhere (MAQC Consortium, 2006), suggesting the reliability of the assay system. To verify the results obtained from the microarray assay, we further achieved expression analyses by RT–PCR and Northern blotting on the candidate transcripts screened from the first single microarray in the individual, but not pooled, samples.

Quantitative RT–PCR

Total RNA was extracted from tissues using the RNeasy Midi kit and was DNase-treated (RNase-Free DNase set; Qiagen, USA). Total RNA (1–2 μg) was reverse-transcribed with an Oligo(dT)$_{20}$ primer using Superscript III RT (Invitrogen, USA). Real-time quantitative PCR was performed on a LightCycler (Roche Diagnostics, Germany) using a SYBR Premix Ex Taq kit (Takara Bio, Japan) according to the manufacturer's protocol. The expression levels of individual genes were normalized to that of glyceraldehyde-3-phosphate dehydrogenase (GAPDH). Relative mRNA abundance of each gene was calculated and verified using the standard curve method (Applied Biosystems, USA). In some experiments in order to examine the open reading frame of *Lmod2*

Table 1. Primer sequences for the real-time and semi-quantitative RT–PCR

Official symbol of gene	Genbank accession no.	Bases spanned	Sense primer (5′ to 3′)	Antisense primer (3′ to 5′)
Real-time quantitative PCR				
Lmod2	AB331240	1545–1645	5′-AATGGAAGAAAGCTCCCGG-3′	5′-CCACCCTCCGTAGCTGTCTTAT-3′
Tmod1	NM_013044	2330–2437	5′-GACAGTGATGGCTCAAAAGCTG-3′	5′-CGATGCCACTCTAGTTACCCTG-3′
Tmod2	BF567833	116–243	5′-CGTTTCCGTTAACCATATCCG-3′	5′-TGTACAAGCCACCAAGCGTGT-3′
GAPDH	NM_017008	1457–1714	5′-ACATCATCCCTGCATCCACT-3′	5′-GGGAGTTGCTGTTGAACTCA-3′
Semi-quantitative RT–PCR				
Lmod2	AB331240	19–1668	5′-ATGTCTACATTTGGCTACAGAAGGGG-3′	5′-CTATCTCAGAGCTTCGGGAACTTC-3′

In real-time PCR in order to determine the subregional distribution in the brain, the reaction products were separated in 10% polyacrylamide gel electrophoresis in 1× TBE (89 mM Tris–borate and 2 mM EDTA) and visualized by staining with SYBR Green I. PCR was performed under the conditions of annealing temperature at 55 °C for 30 cycles (*Lmod2*), for 26 cycles (*Tmod1*), for 25 cycles (*Tmod2*), and for 22 cycles (*GAPDH*), respectively. In the semi-quantitative RT–PCR, the PCR products were electrophoretically separated on 1.5% agarose gel in 1× TAE (40 mM Tris–acetate and 1 mM EDTA) and visualized by staining with ethidium bromide. After 100 times dilution of each cDNA, PCR was performed under the condition of annealing temperature at 55 °C for 35 cycles.

mRNA and the expression levels in the thalamus and heart, semi-quantitative RT–PCR was performed on GeneAmp PCR system 9700 (Applied Biosystems) using KOD DNA polymerase (Japan). The primer sequences for these experiments are shown in Table 1.

Northern blot analysis

Two micrograms of poly(A)$^+$ RNA purified from the rat thalamus using an oligo(dT)-cellulose column (Amersham, UK) was separated by formaldehyde/1.0% agarose gel electrophoresis and transferred to a Hybond-XL membrane (Amersham). A 335-bp cDNA fragment corresponding to the nucleotide position 1549-1883 of rat *Lmod2* cDNA (DDBJ accession no. AB331240) was subcloned into pGEM-T Easy Vector (Promega). Plasmids were linealized, and digoxigenin (DIG)-labelled RNA probes were prepared by *in-vitro* transcription using T7 and SP6 RNA polymerases. Prehybridization and hybridization were performed in DIG-Easy Hyb buffer (Roche) at 68 °C for 2 h and overnight, respectively. The membranes were washed in 2× SSC/0.1% SDS at room temperature for 1 h and in 0.1× SSC/0.1% SDS at 68 °C for 1 h. The hybridized probes were immunodetected with anti-DIG antibody conjugated with alkaline phosphatase (AP) and visualized with a chemiluminescence substrate, CDP-Star (Roche). In some experiments, Rat Multiple Tissue Northern (MTN) Blot (Takara Bio/Clontech) was used for hybridization.

Internal standard housekeeping gene for Northern blot and RT–PCR analyses

In the present study we routinely used β-actin expression for the normalization of expression levels of subject genes in the different organs or brain areas in Northern blot analyses in adult rats. Because the basal expression of β-actin, but not GAPDH, has been found to be altered in the developing rat brain whilst PCP does not affect brain expression of the two genes in the adult period, GAPDH was selected as an internal standard housekeeping gene when studying developmental changes in PCP induction of the *Lmod2* gene by RT–PCR techniques.

In-situ *hybridization*

In-situ hybridization histochemistry was performed on coronal or sagittal brain sections according to the methods of Kiyama's research group. For *in-situ* hybridization studies using DIG-labelled RNA probes (nt 1549-1883, Genbank accession no. AB331240) (Nagata *et al.* 2006; Ohba *et al.* 2004), slide-mounted frozen brain sections (16-μm-thick) were briefly dried, fixed in 4% paraformaldehyde in PBS for 20 min, rinsed with PBS for 2 × 15 min, and treated with 5× SSC for 15 min. To detect *Lmod2* mRNA signals following the pre-hybridization and hybridization procedures (see legend of Fig. 4*c–e*), the sections were shortly rinsed in buffer 3 [100 mM Tris–HCl (pH 9.5), 150 mM NaCl, 50 mM $MgCl_2$], and incubated in buffer 3 containing NBT (Nitro Blue tetrazolium)/BCIP

Table 2. Screening of the developmentally regulated PCP-responsive transcripts in the rat thalamus by DNA microarray

Gene name	Genbank accession no.	PD 50		PD 8	
		Log_2 ratio (% of control)	Change p value	Log_2 ratio (% of control)	Change p value
Fos: FBJ murine osteosarcoma viral oncogene homolog	BF415939	2.1 (428)	0.00002	0.2 (115)	0.35
Klf2_predicted: Kruppel-like factor 2 (lung) (predicted)	BF288243	1.6 (303)	0.00002	0.2 (115)	0.5
Nr4a3: Nuclear receptor subfamily 4, group A, member 3	NM_031628.1	1.4 (264)	0.00002	0.1 (107)	0.5
Klf4: Kruppel-like factor 4 (gut)	NM_053713.1	1.4 (264)	0.00002	−0.3 (77)	0.5
LOC296935: Similar to leiomodin 2 (cardiac)	AI453854	1.1 (214)	0.000214	Absent	

The thalamic expression of >30 000 clones was analysed by the Affymetrix Rat Genome 230 2.0 arrays (Affymetrix, USA) in the young adult (PD 50) and infant (PD 8) rats 60 min after acute s.c. administration of PCP (7.5 mg/kg) or saline. The microarrays were scanned with the GeneChip Scanner 3000 and analysed using the GeneChip operating software version 1.2. We used moderately stringent cut-off indices for significance determination (McClung & Nestler, 2003): genes were considered to be detected if the experimental or control signal was $\geqslant 20$ (detection p value $\leqslant 0.04$) and were considered to be up-regulated if the log_2 ratio experimental value/control value for each gene was $\geqslant 1.0$ ($\geqslant 200\%$ of control value, change p value $\leqslant 0.002$). We screened the transcripts of the known genes that showed the up-regulation by PCP injection with the log_2 ratio experimental (PCP)/control (saline) of >1.0 (change p value $\leqslant 0.002$) at PD 50 and no significant changes in the ratio at PD 8. 'Absent' means that the gene expression was not detected (the experimental or control signal was <20, or detection p value <0.04).

(5-bromo-4-chloro-3-indolyl phosphate) stock solution (Roche) overnight for up to 3 d at 4 °C. The colour development was terminated by TE [10 mM Tris–HCl (pH 7.4), 1 mM EDTA].

For radioisotope-labelled *in-situ* hybridization experiments (Tanabe *et al.* 1998, 1999), ^{35}S-labelled cRNA probes (nt 1549-1883, GenBank accession no. AB331240) were prepared by *in-vitro* transcription using T7 and SP6 RNA polymerases and [α-^{35}S]UTP (Amersham, 37 TBq/mmol). The brain sections were dried, fixed in 4% paraformaldehyde in phosphate buffer for 20 min at room temperature, treated with 10 μg/ml proteinase-K in 50 mM Tris–HCl (pH 8.0), and 5 mM EDTA for 5 min, and then fixed again. To detect the hybridized ^{35}S-labelled cRNA probes following the hybridization procedures (see Fig. 4*b* legend), the sections were exposed to an X-ray film (BioMax XAR, USA) for 1 wk and subjected to autoradiography.

Statistical analysis

Results are given as means with S.E.M. of the data. Statistical differences among three groups or more with parametric and non-parametric distribution were estimated by the Kruskal–Wallis test followed by the Scheffé *post-hoc* test. Some developmental and organ differences in the effects of PCP were examined by a two-way ANOVA followed by the Scheffé *post-hoc* test. We confirmed by Bartlett test that the datasets analysed with the two-way ANOVA had a parametric distribution.

Nucleotide sequences

The DDBJ/GenBank/EMBL accession number for primary nucleotide sequence of rat *Lmod2* is AB331240.

Results

Detection of Lmod2 mRNA as a developmentally regulated PCP-responsive transcript by a DNA microarray method

From the DNA microarray data, we screened the thalamic transcripts of the known genes that showed up-regulation by PCP injection (7.5 mg/kg s.c.) with the log_2 ratio experimental PCP/control (saline) of >1.0 [>2-fold (200% of control)] with a statistical significant p value at PD 50 (young adult rat) and no significant changes in the ratio at PD 8 (infant rat). The filtering procedure provided us with five candidate transcripts: c-*fos*, Klf2, Nr4a3, Klf4 and leiomodin2 (*Lmod2*)-like (Table 2). Because there has been no study on the expression, functions and neuronal or psychiatric involvement of the *Lmod2* (or *Lmod2*-like) gene in the brain, whereas other genes have already been reported to be regulated by PCP in the rat brain (Kaiser *et al.* 2004), we characterized the structural, developmental, pharmacological and neuroanatomical properties of the *Lmod2/Lmod2*-like transcript.

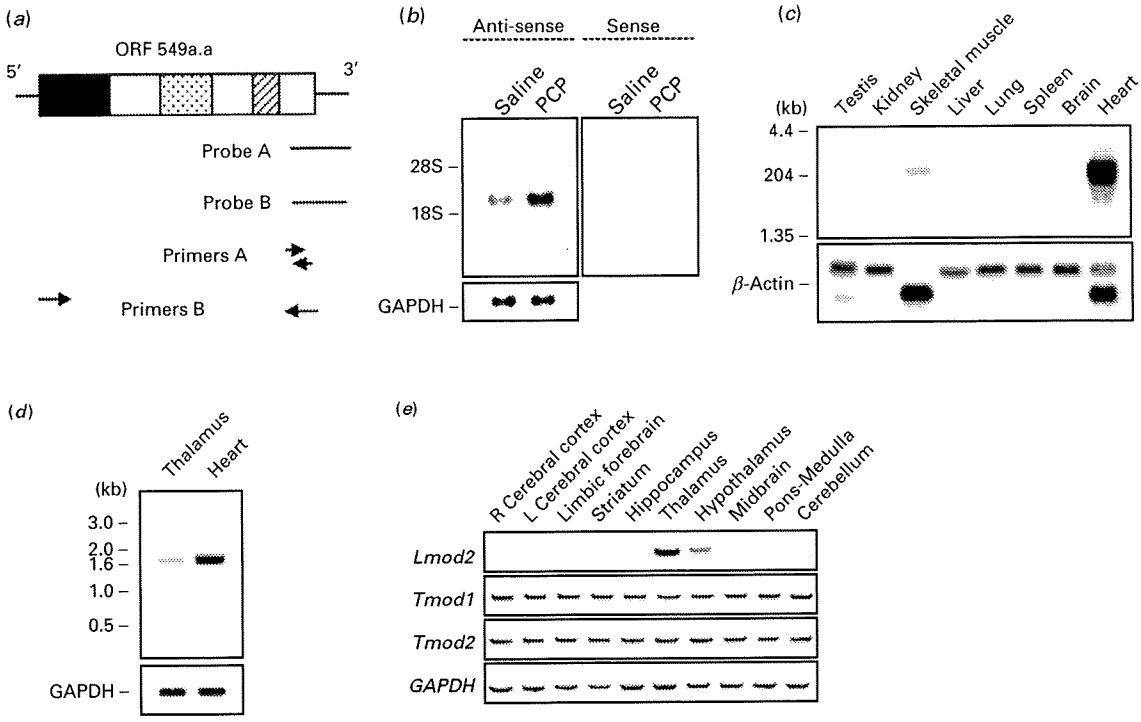

Fig. 1. Cloning and expression of rat *Lmod2*. (*a*) Schematic representation of the structure of rat *Lmod2* cDNA and the nucleotide sequences encoding the open reading frame (ORF). Domains and motifs: closed box, possible tropomyosin-binding domain; dotted box, leucine-rich repeats; hatched box, polyproline motif. Bars and arrows underneath indicate the positions of probes and primers used for the following purposes of experiments: probe A, microarray hybridization (probe name: 1377610_at, ID: RAG230_2_10158); probe B, Northern hybridization and *in-situ* hybridization; primer set A, real-time RT–PCR; primer set B, isolation and determination of the ORF of rat *Lmod2*. (*b*) Northern blot analyses of the poly(A)$^+$ RNAs (2 μg/lane) from the thalamus of the adult rat treated with saline or PCP (7.5 mg/kg s.c.). Hybridization with a selective probe to *Lmod2* mRNA against the sequence of nt 1549-1883 [probe B in panel (*a*)] recognized a single band in each lane. (*c*) Tissue distribution of *Lmod2* mRNA analysed by Northern blot of poly(A)$^+$ RNAs (2 μg/lane) from various organs of the adult rat with probe B in panel (*b*). The signal detected in the rat heart and skeletal muscles was the same size as that detected in the thalamus. (*d*) Semi-quantitative RT–PCR analysis of basal *Lmod2* mRNA expression in the thalamus and heart of the adult rat. The same PCR products, which were amplified by primer B in panel (*a*), were detected at 1.6 kb in both the thalamus and heart. (*e*) Semi-quantitative RT–PCR analysis of the basal expression of *Lmod2*, *Tmod1*, *Tmod2* and GAPDH mRNAs in the discrete brain areas of the adult rat. The positions of primer sets used for the amplification of cDNA are described in detail in Table 1.

To this end, we first screened *Lmod2/Lmod2*-like cDNAs from the adult rat thalamus by RT–PCR with the primer set designed based on mouse *Lmod2* cDNA (Genbank accession no. NM_053098) and the rat genomic sequence database (Fig. 1*a*). The isolated rat *Lmod2/Lmod2*-like cDNA is predicted to encode a protein with a molecular weight of 64.5 kDa that is composed of 549 amino acids showing 97% identity with mouse Lmod2 protein (Genbank accession no. NM_444328, originally designated as C-Lmod protein; Conley *et al.* 2001). Thus, we concluded that this gene product was a rat ortholog of the mouse Lmod2 protein. *Lmod2* is thought to be a member of the tropomodulin (Tmod) family of the actin filament pointed end-capping proteins (Fischer & Fowler, 2003), The structures of the presumed tropomyosin-binding (TM) domain and leucine-rich repeats (LLR), which were characteristic of the Tmod protein family, were well conserved in rat Lmod2 protein (Fig. 1*a*), suggesting the possible interaction with the other molecules that might regulate actin-cytoskeletal structures (Conley *et al.* 2001; Fischer & Fowler, 2003). The polyproline (PP) motif near the carboxyl terminal, which was similar to that of Lmod1, is also reserved in rat Lmod2 protein. Additionally, we detected a possible nuclear localization signal (NLS), whose amino-acid sequences are RKKK (480-483; mouse, 481-484), in Lmod2 protein using the PSORTII program (Nakai & Horton, 1999). A similar NLS was reported in Tmod proteins (Kong & Kedes, 2004) but was absent in Lmod1. However, rat Lmod2 protein did not possess a typical nuclear export signal motif, which was identified in Tmod proteins (Kong & Kedes, 2004).

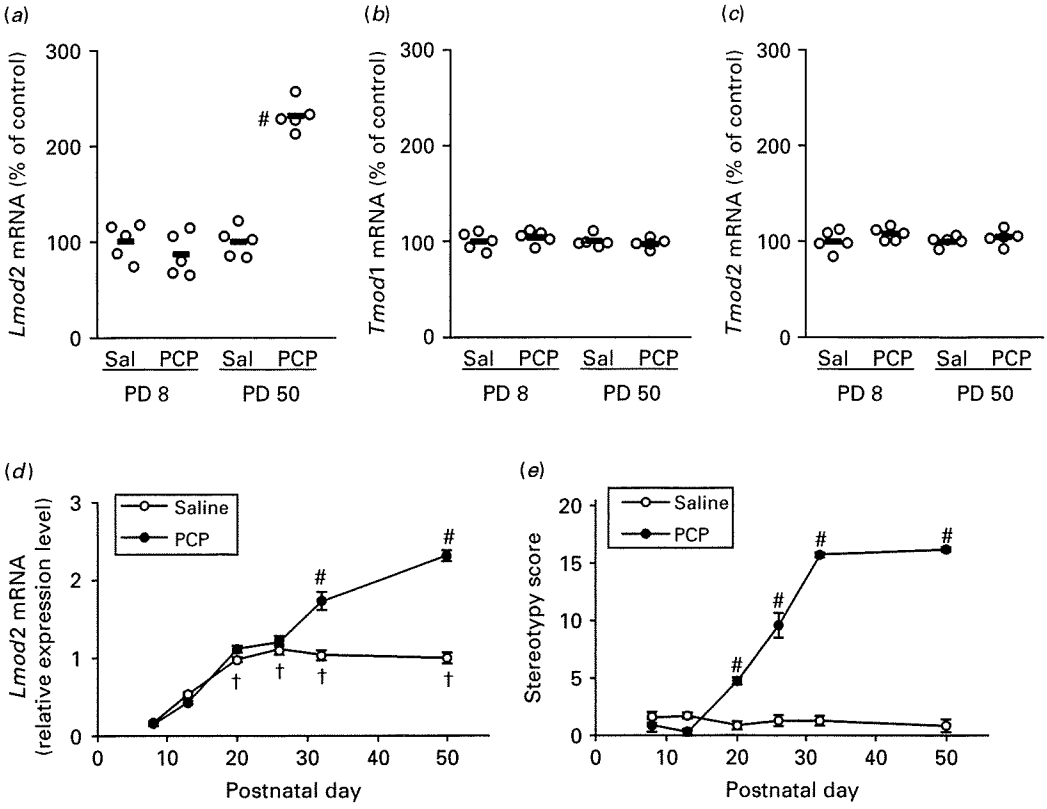

Fig. 2. Effects of acute PCP injection on expression of *Lmod2*, *Tmod1* and *Tmod2* mRNAs in the thalamus and behaviour in developing rats. Relative expression levels of *Lmod2*, *Tmod1* and *Tmod2* mRNAs (*Lmod2*, *Tmod1* or *Tmod2* to GAPDH mRNA ratio) were determined by the real-time RT–PCR method 60 min after administration of PCP or saline. Results are the means with S.E.M. of data obtained from five rats per group and are expressed as a percentage of the values of the adult (PD 50) saline-treated animals. (*a*) *Lmod2*: adult rats (PD 50), saline 100±8%, PCP 231±7%$^{\#}$ ($^{\#}$ $p<0.01$ *vs.* saline-treated controls); infant rats (PD 8), saline 100±8%, PCP 87±10 ($p>0.05$ *vs.* saline-treated controls; Scheffé test) (two-way ANOVA, postnatal days effect: $F_{1,16}=76.878$, $p<0.0001$; PCP treatment effect: $F_{1,16}=51.066$, $p<0.0001$; postnatal days × PCP treatment effect: $F_{1,16}=77.456$, $p<0.0001$). (*b*) *Tmod1*: adult rats (PD 50), saline 100±3%, PCP 97±2 ($p>0.05$ *vs.* respective saline-treated controls); infant rats (PD 8), saline 100±4%, PCP 104±3% ($p>0.05$ *vs.* respective saline-treated controls; Scheffé test) (two-way ANOVA, postnatal days effect: $F_{1,16}=0.981$, $p=0.34$; PCP treatment effect: $F_{1,16}=0.047$, $p=0.83$; postnatal days × PCP treatment effect: $F_{1,16}=0.944$, $p=0.35$). (*c*) *Tmod2*: adult rats (PD 50), saline 100±2%, PCP 104±2% ($p>0.05$ *vs.* the respective saline-treated controls); infant rats (PD 8), saline 100±5%, PCP 107±3% ($p>0.05$ *vs.* the respective saline-treated controls; Scheffé test) (two-way ANOVA, postnatal days effect: $F_{1,16}=0.241$, $p=0.63$; PCP treatment effect: $F_{1,16}=2.546$, $p=0.13$; postnatal days × PCP treatment effect: $F_{1,16}=0.228$, $P=0.64$). (*d*) Rats at PD 8, 13, 20, 26, 32 and 50 were treated with 7.5 mg/kg PCP subcutaneously and the relative expression levels of *Lmod2* mRNA (*Lmod2*:GAPDH mRNA ratio) were determined by the real-time RT–PCR method 60 min after administration of PCP or saline. Results are the means with S.E.M. of data obtained from five or six rats per group and are expressed as a percentage of the values of the adult (PD 50) saline-treated animals ($^{\#}$ $p<0.01$ *vs.* respective saline-treated controls; † $p<0.01$ *vs.* saline-treated rats at PD 8). (*e*) The intensity of the PCP-induced stereotypy was evaluated by the following stereotyped behavioural rating scale from 30 to 60 min after drug administration: 0, no stereotyped behaviour; 1, increased exploratory activity with occasional sniffing, grooming or rearing; 2, episodic non-directional movement, weaving, reciprocal forepaw treading, higher frequency of sniffing, grooming or rearing >1; 3, intermittent turning, backpedalling and weaving with or without bursts of frequent sniffing, grooming or rearing; 4, rapid and continuous turning, backpedalling, weaving, sniffing and gagging; and 5, dyskinetic extension and flexion of limbs, head and neck. Results are the means with S.E.M. of data obtained from five to seven rats per group ($^{\#}$ $p<0.01$ *vs.* respective saline-treated controls).

On the Northern blot of the 2 μg poly(A)$^+$ RNA from the thalamus of adult rats, we detected a single transcript at 2.4 kb with an RNA probe in an anti-sense specific manner (Fig. 1*b*). This signal was up-regulated in the adult rat thalamus by PCP administration in agreement with the results of the DNA microarray

assay. The intense signal of rat *Lmod2* mRNA was predominantly observed in the heart at an extremely high level, followed by the skeletal muscle at a low level but was not detectable in the whole brain tissue at 2 μg poly(A)$^+$ RNA (Fig. 1*c*). This distribution pattern was similar to that of human *Lmod2* reported previously (Conley *et al.* 2001).

Using RT–PCR with several different primer sets (Fig. 1*a*), we confirmed that *Lmod2* RNA expressed in the thalamus shares essentially the same primary structure with that in the heart of the rat. This conclusion was obtained by the results in which, in both the thalamus and heart, the identical PCR products of the 1647 bp nucleotide sequence that contains the same open reading frame of *Lmod2* were detected as a single band, while the heart expressed much higher levels of *Lmod2* transcripts than the thalamus (Fig. 1*d*). Moreover, the semi-quantitative RT–PCR analysis revealed that *Lmod2* mRNA was exclusively expressed in the thalamus and detected at low levels in the hypothalamus and midbrain among the discrete brain areas of the adult rat, while *Tmod1* and *Tmod2* mRNAs were evenly distributed throughout the brain regions examined (Fig. 1*e*).

Effects of acute PCP on expression of Lmod2 transcripts in the thalamus and behaviour in developing rats

The contrasting responses to PCP between PD 8 and 50 in the thalamus as shown by DNA microarray analysis were semi-quantitatively verified by the real-time RT–PCR method. As indicated in Fig. 2*a*, PCP treatment (7.5 mg/kg s.c.) caused a significant increase in the ratios of mRNA levels of *Lmod2* to those of GAPDH compared to the saline-treated controls in adult rats but no significant changes were seen in infant rats. In contrast, the relative thalamic expressions of other *Tmod* family genes, *Tmod1* (Fig. 2*b*) and *Tmod2* (Fig. 2*c*), at PD 8 and 50 were not affected by the acute injection of PCP. The similar magnitude of an increase in thalamic *Lmod2* expression after PCP injection in the present microarray using the pooled cDNA (% of saline-treated control value: *Lmod2*, 214%) and RT–PCR (*Lmod2*, 231%; Fig. 2*a*) assay using the individual samples adds further reliability to the microarray analysis.

To further clarify the postnatal developmental changes in the basal and PCP-induced expression of thalamic *Lmod2*, we evaluated the effects of a single injection of saline and PCP (7.5 mg/kg) on the relative mRNA levels of the gene 1 h later at PD 8, 13, 20, 24, 32 and 50. The expression after saline administration (or basal expression) gradually increased in the thalamus of the rat with postnatal days up to PD 20 and then continued at a plateau level thereafter. Acute PCP failed to alter *Lmod2* mRNA levels at PD 8, 13, 20 and 24 but significantly augmented the transcript expression at PD 32 and 50 (Fig. 2*d*).

The same dose of PCP produced a statistically significant increase in the stereotypy scores at PD 20, 26, 32 and 50, but not at PD 8 and 13, and a similar intensity of the abnormal behaviour was seen between PD 32 and 50 (Fig. 2*e*). These behavioral observations indicated that the apparent adult type stereotypy (behavioural changes) after acute PCP injection seems to occur between PD 26 and PD 32.

In the young adult period, thalamic *Lmod2* mRNA expression in adult rats (PD 50) increased rapidly, peaked at 1–3 h and returned to the saline-treated levels within 6 h after acute PCP (7.5 mg/kg s.c.) administration (Fig. 3*a*). However, there were no changes in *Lmod2* mRNA levels in the thalamus of the infant rats (PD 8) up to 6 h post-injection. The time-course of PCP-induced thalamic *Lmod2* up-regulation and stereotypy in the adult rats appears to be parallel (Fig. 3*a*, *b*).

Effects of acute PCP injection on expression of Lmod2 transcripts in the heart and brain regions of adult rats as revealed by RT–PCR and in-situ *hybridization*

Unlike *Lmod2* expression in the thalamus, the gene transcript levels in the heart were unaffected by acute injection of PCP (7.5mg/kg s.c.) in adult rats (Fig. 4*a*). Further, we tried to clarify the exact brain or thalamic portions where PCP up-regulates *Lmod2* gene expression using an *in-situ* hybridization method. In accordance with the RT–PCR data, *Lmod2* mRNA signals were found to be restricted to the thalamus in the saline-treated control rats at PD 50, although the signal intensity was low (Fig. 4*b*, left panel). Acute PCP treatment (7.5 mg/kg s.c.) augmented thalamic *Lmod2* expression without apparent influence on its basal distribution pattern (Fig. 4*b*, right panel). Therefore, we intensively performed *in-situ* hybridization studies on the brain samples obtained from PCP-treated adult rats.

With a DIG-labelled anti-sense RNA probe, *Lmod2* mRNA signals were observed in the anterior nucleus and the lateral nucleus of the thalamus as shown in the sagittal sections (Fig. 4*c*, *d*). In the brain sections counterstained by Methyl Green at higher magnification, the *Lmod2* mRNA signal was mainly detected in the cells that possessed a neuron-like morphological

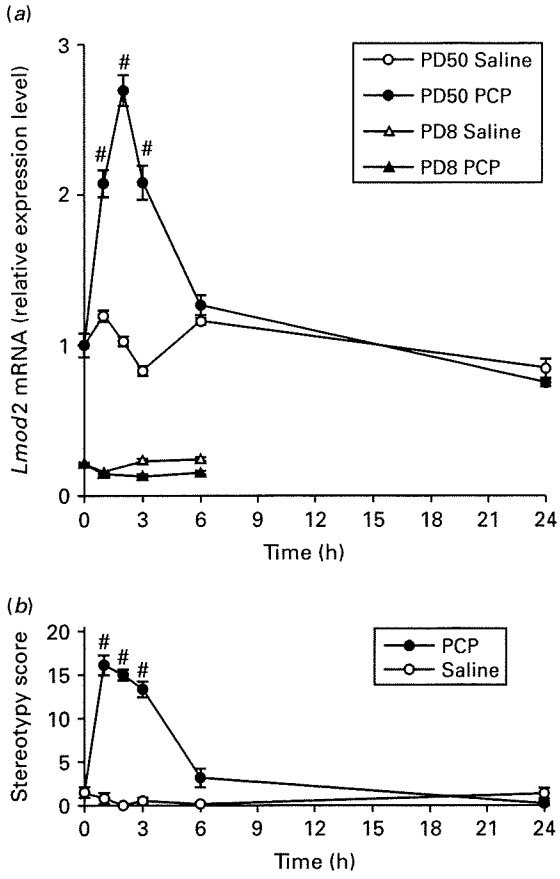

Fig. 3. Time-course of thalamic *Lmod2* mRNA expression and behavioural changes after acute PCP injection in adult or infant rats. (*a*) Relative expression levels of *Lmod2* mRNA in the thalamus of adult (PD 50) and infant (PD 8) rats (*Lmod2*:GAPDH mRNA ratio) were assayed by real-time RT–PCR at various times after acute PCP administration (7.5 mg/kg s.c.). The expression levels at time 0 were determined in the animals prior to the treatment. Results are the means with S.E.M. of data obtained from five or six rats per group and are expressed as a percentage of the values of the adult (PD 50) saline-treated animals ($^{\#}p<0.01$ *vs.* respective saline-treated controls). (*b*) Stereotypy scores after acute PCP administration. The cumulative behavioural scores as the summation of each 10-min score are evaluated by the rating scale described in the legend of Fig. 2*b* and shown as the means with S.E.M. of the data obtained from six rats in each group ($^{\#}p<0.01$ *vs.* respective saline-treated controls).

feature with a characteristic large round-shaped nucleus (Fig. 4*e*). A more sensitive *in-situ* hybridization detection system with a ^{35}S-labelled anti-sense RNA probe revealed that strong hybridization signals of *Lmod2* mRNA were predominantly observed in the rostral areas of the thalamus including the anterior thalamic complex [i.e. the anteromedial (AM), anteroventral (AV), and inter-anteromedial (IAM) nucleus], and the ventral anterior-lateral complex (Fig. 4*f–l*). In addition, much lower hybridization signals were found in limited areas of the caudal thalamus including the ventral medial nucleus, the rhomboid nucleus, the intralaminar thalamic nucleus [consisting of the central medial (CM), paracentral (PCN), and central lateral (CL) nucleus], and the lateral and ventral posterior complex of the thalamus. No hybridization signal was detected in any brain sections studied with the corresponding sense probe (Fig. 4*m*).

Effects of acute injection of NMDA receptor antagonists, dopamine agonist and antagonist on expression of Lmod2 transcripts in the thalamus of adult rats

Because *Lmod2* has been detected as a novel candidate for a schizophrenia symptom-related gene in the present study, we evaluated the effects of different psychotomimetics, PCP, dizocilpine and methamphetamine, on thalamic *Lmod2* mRNA expression in adult rats. The acute injection of another non-competitive NMDA receptor antagonist, MK-801 (0.5 mg/kg s.c.), mimicked the up-regulation of the thalamic expression levels of *Lmod2* mRNA seen following PCP administration (7.5 mg/kg s.c.) (Fig. 5*a*). An indirect dopamine agonist, methamphetamine (MAP, 4.8 mg/kg s.c.) produced a smaller significant increase in *Lmod2* mRNA levels than PCP and MK-801 (Fig. 5*a*).

We also examined the effects of Hal, which is a D_2-selective dopamine receptor antagonist, on basal expression and PCP-induced up-regulation of *Lmod2* mRNA. Pretreatment with haloperidol (1.0 mg/kg i.p.) 30 min before PCP injection partially antagonized the ability of PCP to augment *Lmod2* mRNA expression (Fig. 5*b*). Hal, by itself, showed no significant effect on *Lmod2* mRNA expression.

Discussion

By using a DNA microarray technique, we show that *Lmod2* is a developmentally regulated and PCP-regulated gene in the rat thalamus in that a schizophrenomimetic respectively causes no and prominent up-regulation of thalamic *Lmod2* gene expression in infant (PD 8) and young adult (PD 50) rats. The significant increase in thalamic *Lmod2* mRNA expression after PCP administration is observed only after PD 32. We further demonstrate that the basal and PCP-induced expression of *Lmod2* is confined to the anterior and lateral nuclei of the thalamus in the brain. The up-regulation of thalamic *Lmod2* transcripts in the

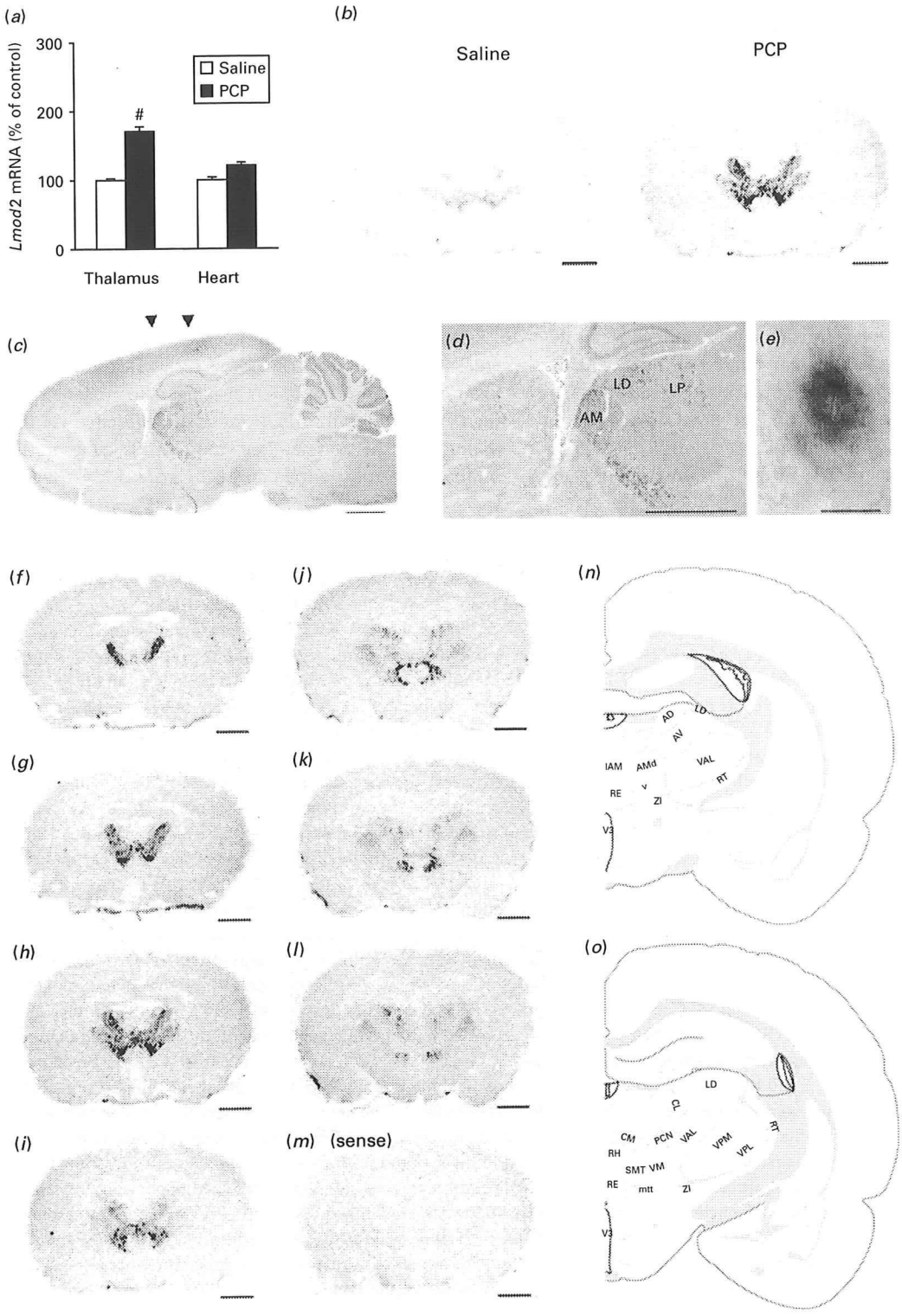

COLOUR

Fig. 4. Effects of acute PCP injection on *Lmod2* mRNA expression in the heart and brain regions of adult rats. (*a*) Relative expression levels of *Lmod2* mRNAs (*Lmod2*:GAPDH mRNA ratio) were determined by the real-time RT–PCR method in the thalamus and heart of the adult (PD 50) rat 60 min after administration of PCP (7.5 mg/kg s.c.) or saline. Results are the means with S.E.M. of data obtained from five rats per group and are expressed as a percentage of the values of the respective saline-treated controls. Thalamus: saline 100±3%, PCP 171±7$^{\#}$ ($^{\#}$ $p<0.01$ *vs.* saline-treated controls); heart: saline 100±4%, PCP

adult period is totally and partly mimicked by other schizophrenomimetics, dizocilpine and MAP, respectively, and moderately attenuated by the D_2-preferring dopamine receptor antagonist Hal. These developmental, neuroanatomical and pharmacological profiles of *Lmod2* responses suggest that *Lmod2* and its protein products could, at least in part, be associated with the late-developing onset and the specific neuron circuits for the adult type of PCP-induced abnormal behaviour in the rat.

This is the first study to indicate the profound influence of psychotomimetics on brain mRNA expression of the *Lmod2* gene. The Tmod gene family member has so far been considered to represent the muscular tissue-selective expression without its transcripts in the brain. However, we have demonstrated that considerable amounts of *Lmod2* mRNAs are predominantly concentrated in the thalamus among the brain tissues. The expressional changes in the thalamic *Lmod2* by psychotropic drugs may imply the possible involvement of the molecule in the regulation of psychological and motor functions. This assumption appears to be supported by the similar time-course in up-regulation of *Lmod2* expression and stereotyped behaviour after PCP (Fig. 3*a*, *b*). On the other hand, the present study also revealed the obvious discrepancy between the postnatal development of the above molecular and behavioural responses to PCP (Fig. 2*d*, *e*). Thus, the exact regulatory roles of the gene await further elucidation.

The possibility that the post-weaning marked increase in *Lmod2* transcript levels by PCP could be due to a non-specific phenomenon appears to be denied by the observations that PCP failed to influence (1) the thalamic expression of other Tmod family genes in the infant and adult periods and (2) *Lmod2* mRNA levels

---

121 ± 4 ($p > 0.05$ *vs.* saline-treated controls, n.s., no significant difference) (two-way ANOVA, organ effect: $F_{1,16} = 25.109$, $p < 0.001$; PCP treatment effect: $F_{1,16} = 85.035$, $p < 0.0001$; organ × PCP treatment effect: $F_{1,16} = 24.988$, $p < 0.001$). (*b*) Thalamic region-restricted *Lmod2* mRNA expression in the adult rat (PD 50) brain 60 min after acute PCP administration (7.5 mg/kg s.c.) as revealed by *in-situ* hybridization histochemistry with ^{35}S-labelled RNA probe for *Lmod2*. Both of the basal (saline-treated control animals) and PCP-induced *Lmod2* mRNA signals were confined to the thalamic regions in the brain (scale bars, 2 mm). For the radiolabelled *in-situ* hybridization, the slide-mounted fixed brain sections were rinsed in distilled water and then acetylated with 0.25% acetic anhydride in 0.1 M triethanolamine. After rinsing in PBS, the sections were dehydrated in an ascending ethanol series (70%, 95%, and 100%), defatted in chloroform, rinsed in ethanol, and air-dried. Radiolabelled probes (4×10^7 cpm per slide) in hybridization buffer [50% deionized formamide, 0.3 M NaCl, 20 mM Tris–HCl (pH 8.0), 5 mM EDTA, 10 mM PBS, 10% dextran sulfate, 1× Denhardt's solution, 0.2% sarcosyl, 500 μg/ml yeast transfer RNA, and 200 μg/ml salmon sperm DNA] were denatured for 5 min at 80 °C, quenched on ice, and placed on the sections. Hybridization was performed overnight at 55 °C in a humid chamber. Hybridized sections were rinsed briefly in 5× SSC and 1% 2-mercaptoethanol at 55 °C and washed in 50% deionized formamide, 2× SSC, and 10% 2-mercaptoethanol (high-stringency buffer) for 30 min at 65 °C. After rinsing the sections in RNase buffer [0.5 M NaCl, 10 mM Tris–HCl (pH 8.0), and 1 mM EDTA], they were treated with 1.0 μg/ml RNase-A in RNase buffer for 30 min at 37 °C, and washed in RNase buffer. The sections were then incubated in high-stringency buffer as described above, rinsed in 2× and 0.1× SSC for 10 min each at room temperature, dehydrated in an ascending ethanol series, and air-dried. mRNA localization was assessed by X-ray film autoradiography. (*c–e*) DIG-labelled *in-situ* hybridization on the sagittal brain sections of 50-d-old adult rat. As a pre-hybridization procedure, the slide-mounted brain sections were incubated for 2 h at 58 °C in hybridization buffer (50% deionized formamide, 5× SSC, and 40 μg/ml salmon sperm DNA). Hybridization of DIG-labelled RNA probes was performed in a humid chamber overnight at 58 °C, and then washed with 2× SSC for 30 min at room temperature, and rinsed in 2× and 0.5× SSC for 60 min each at 55 °C. After rinsing in buffer 1 [100 mM Tris (pH 7.5), and 150 mM NaCl], the sections were incubated for 2 h in buffer 1 and sheep anti-DIG antibody conjugated with alkaline phosphatase and washed twice for 15 min in buffer 1. The *Lmod2* mRNA signals were detected as purple-coloured staining by the DIG-labelled RNA probe, and the cell nuclei are counterstained by Methyl Green as shown in blue. The positions of the two arrowheads in panel (*c*) correspond to those of the respective coronal sections represented in panels (*f*) (rostral) and (*l*) (caudal). Scale bars: (*c*, *d*) 2 mm; (*e*) 20 μm. Abbreviations: (*d*) AM, Anteromedial nucleus; LP, lateral posterior nucleus; LD, lateral dorsal nucleus. (*f–l*) *In-situ* hybridization with ^{35}S-labelled RNA probe for *Lmod2* on the coronal brain sections of the 50-d-old adult rat at levels of the thalamic regions. The sections are aligned in the orientation from caudal to rostral. (*f–l*) Positions of panels (*f*) and (*l*) are represented in panel (*c*). The details of the experimental procedures of radiolabelled *in-situ* hybridization are described in the legend of panel (*b*). (*m*) This panel, at the same level as panel (*i*), was hybridized with the corresponding sense probe. Scale bars: (*f–m*), 2 mm. (*n*, *o*) Schematic illustration of the structures of the thalamus at the level of panel *h* (*n*) and panel *j* (*o*). AD, Anterodorsal nucleus; AMd, Anteromedial nucleus, dorsal part; Amv, Anteromedial nucleus, ventral part; AV, anteroventral nucleus; CM, central medial nucleus; CL, central lateral nucleus; IAM, interanteromedial nucleus; LD, lateral dorsal nucleus; mtt, mammillothalamic tract; PCN, paracentral nucleus; RE, nucleus reunions; RH, rhomboid nucleus; RT, reticular nucleus; SMT, submedial nucleus; VAL, ventral anterior-lateral complex; VM, ventral medial nucleus; VPL, ventral posterolateral nucleus; VPM, ventro posteromedial nucleus; V3, third ventricle; ZI, zona incerta.

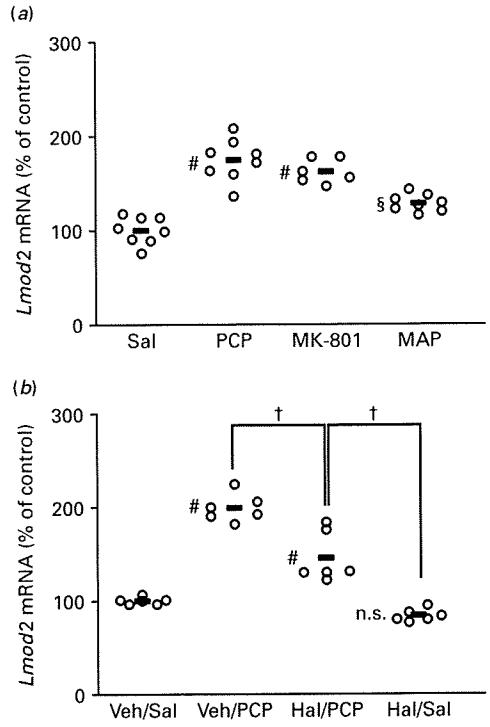

Fig. 5. Effects of acute administration of psychotomimetic and antipsychotic drugs on *Lmod2* mRNA expression in the thalamus. (*a*) Effects of PCP, MK-801 and methamphetamine (MAP) on thalamic *Lmod2* mRNA. Relative expression levels of *Lmod2* mRNA in the thalamus of the adult (PD 50) rat (*Lmod2*:GAPDH mRNA ratio) were assayed by the real-time RT–PCR method 60 min after acute PCP (7.5 mg/kg s.c.), MK-801 (0.5 mg/kg s.c.), and MAP (4.8 mg/kg s.c.) administration. Results are shown as scatterplots with the means of data (*Lmod2*:GAPDH mRNA ratio) obtained from six or eight rats per group and are expressed as a percentage of the values of the saline-treated controls. Saline (Sal) 100±5%, PCP 174±8#, MK-801 162±5#, MAP 128±3 (# $p<0.01$, § $p<0.05$ *vs.* saline-treated controls). (*b*) Effects of pretreatment with haloperidol (Hal) on PCP-induced up-regulation of thalamic *Lmod2* mRNA. The adult (PD 50) rats were pretreated with Hal (1.0 mg/kg, i.p.) or vehicle (Veh) 30 min before PCP or saline (Sal) administration, and the relative expression levels of *Lmod2* mRNA in the thalamus (*Lmod2*:GAPDH mRNA ratio) were assayed by the real-time RT–PCR method 60 min after acute PCP (7.5 mg/kg, s.c.) or saline injection. Results are the means with S.E.M. of data (*Lmod2*:GAPDH mRNA ratio) obtained from six rats per group and are expressed as a percentage of the values of the vehicle-pretreated and saline-injected controls. Vehicle-pretreated saline-injected controls (Veh/Sal) 100±2%, vehicle-pretreated PCP-injected animals (Veh/PCP) 200±6#, Hal-pretreated PCP-injected animals (Hal/PCP) 145±11#, Hal-pretreated saline-injected animals (Hal/Sal) 83±3 (# $p<0.01$ *vs.* Veh/Sal controls; † $p<0.01$ between Veh/PCP and Hal/PCP animals and between Hal/PCP and Hal/Sal animals). n.s., No significant difference. Veh: 0.15% tartaric acid.

in the heart of the adult animal. The ontogenic differences in brain *Lmod2* induction by PCP might solely depend on those in the time-course of the pharmacodynamics of PCP or the general responses of the brain. However, this explanation seems to be contrary to the observation that (1) PCP caused no change in thalamic *Lmod2* transcript levels even up to 6 h post-injection in the infant rat despite the pronounced increase in those of the adult rat during the same time (Fig. 3*a*), and (2) a similar time-course of the acute PCP-induced increase in *c-fos* gene expression was seen in the various brain areas of the rat at PD 8 and 50 (Sato *et al.* 1997).

The PCP-induced thalamus-selective up-regulation is more likely to be associated with a psychotomimetic action generated by reduced NMDA receptor function and excessive dopaminergic transmission because potent schizophrenomimetic drugs, the selective NMDA antagonist MK-801 and the dopamine signal potentiator MAP, caused an elevation in thalamic *Lmod2* expression. However, MAP elicited a smaller magnitude of elevation than PCP and MK-801 (Fig. 5*a*). The selective D_2 dopamine receptor antagonist, Hal, is found to partially attenuate the increasing effects of PCP on *Lmod2* expression. Together with the fact that NMDA receptor blocking results in the augmented cerebral dopaminergic activities (Umino *et al.* 1998), these observations suggest that the mechanisms underlying PCP-induced up-regulation of *Lmod2* expression may consist of NMDA receptor-related D_2 receptor-sensitive and -insensitive components. These pharmacological features allow us to assume that *Lmod2* or its protein products could participate in the molecular cascades that are dysregulated in the dopamine-dependent positive symptoms and NMDA receptor-associated dopamine-uncoupled negative symptoms and cognitive disturbances in PCP psychosis and schizophrenia (Javitt, 2004; Nishikawa *et al.* 1991; Petersen & Stillman, 1978).

From this pharmacological point of view, it is also plausible that the distinct developmental changes in the responses of *Lmod2* to PCP could be attributed to the neuroanatomical and functional development of the NMDA receptor subunits (Watanabe *et al.* 1992) and/or the cerebral dopamine systems (Pérez-Navarro *et al.* 1993) and in turn this transcript might be an excellent marker for the developmental maturation of the response of the thalamus to increased dopaminergic transmission. The acquisition by the *Lmod2* gene of thalamus-selective responsiveness to PCP after the weaning period (Fig. 2*d*) further argues that the maturation of a specific information-processing system in the thalamus containing *Lmod2* transcripts or proteins as its molecular elements might be required for the

PCP-induced up-regulation of *Lmod2*. Such a system could be disturbed in the schizophrenomimetic-induced abnormal behaviour in experimental animals, schizophrenia-like psychosis and schizophrenia.

In fact, the restricted rostral thalamic regions including the anterior and lateral nuclei that show PCP-induced *Lmod2* expression have been found to display aberrant 2-deoxyglucose uptake, activity-dependent gene expression or cerebral blood flow after ketamine, MK-801, PCP and amphetamine application in experimental animals (Duncan *et al.* 1999) and/or humans (Långsjö *et al.* 2003). Furthermore, *in-vivo* neuroimaging studies describe schizophrenia patients exhibiting reduced activation following cognitive tasks (Andrews *et al.* 2005), decreased *N*-acetylaspartate signals in magnetic resonance spectroscopy (Jakary *et al.* 2005), and increased diffusivity of magnetic resonance diffusion tensor imaging (Rose *et al.* 2006) in these thalamic regions. Biochemical and histochemical analyses using post-mortem brains from schizophrenia patients have revealed various changes in the glutamate system such as altered expression of the L-α-amino-3-hydroxy-5-methylisoxazole-4-propionate (AMPA), kainate and NMDA-type ionotropic glutamate receptors (Ibrahim *et al.* 2000) and glutaminase and glutamine synthetase mRNA (Bruneau *et al.* 2005) in the above *Lmod2*-associated nuclei. Dopaminergic imbalance has also been noted in the thalamus of schizophrenia patients while the major observations concerning the imbalance concentrate on the mediodorsal and posterior nuclei (Takahashi *et al.* 2006).

The series of thalamic aberrations in schizophrenia and its pharmacological models, and the glutamate and dopamine signal-related, late-developing and thalamus-specific nature of the PCP-induced modification of *Lmod2* reinforce the hypothesis that *Lmod2*-expressing cells might compose a part of the information-processing system or neuron circuitry that is specifically distorted in schizophrenia. Accordingly, detection of the schizophrenomimetic-induced *Lmod2* mRNA signals might be a useful tool for tracing the cells and circuits that play a central role in the pathogenesis or pathophysiology of schizophrenia. Because the distribution pattern of *Lmod2* mRNA is similar to that of [^{3}H]muscimol binding to the $GABA_A$ receptor in the thalamic area of the adult rat (Palacios *et al.* 1981), it would be useful to clarify the glutamate–dopamine–GABA interaction in *Lmod2*-expressing cells that is thought to be dysregulated in schizophrenic brains (Lisman *et al.* 2008).

The molecular and functional consequences and the pathophysiological significance of the schizophrenomimetic-induced changes in thalamic *Lmod2* expression are still unknown. Although the biological roles of *Lmod2* protein in brain tissue have not yet been analysed, the characteristic motifs and domain structures of the Lmod2 protein buttress its potential contributions to neuronal and mental functions. Similar to other Tmod family members, the Lomod2 protein has been shown to regulate the organization of the actin-cytoskeletal system through the tropomyosin-binding domain and leucine-rich repeats. A body of evidence has accumulated indicating that actin-based morphological changes in the dendritic spines are involved in synaptic plasticity, which is one of the most essential neural processes for higher brain functions, e.g. learning and memory (Carlisle & Kennedy, 2005).

The polyproline motifs, which the Lmod2 protein possesses at its carboxy-terminal, have been considered to interact with the Src-homology 3 (SH3) domains that are implicated in synaptic organization or reorganization (Segura *et al.* 2007). Moreover, the nuclear localization signal-like amino-acid sequence was found in Lmod2 protein (see Results section). This could be extrapolated to the idea that the possible intranuclear link between Lmod2 and actin could join the integration of gene expression in the thalamus, because nuclear actin has recently been demonstrated to be required for the chromosomal movement that may be connected to the positioning of genes within the nuclear volume for the appropriate transcriptional activity (Dundr *et al.* 2007).

As a consequence, we can presuppose that the quantitative or structural alterations of thalamic *Lmod2* mRNA or proteins would lead to disintegrated synaptic transmission and/or plasticity that may underlie the characteristic symptoms of schizophrenia and related psychoses. Although no studies identified the expressional changes in the mRNA or protein of this gene in schizophrenic brain tissues, and regions of the human genome in which *LMOD2* is located (7q31.32) have not been suggested to be associated with an altered risk of schizophrenia, it would be valuable to investigate the possible involvement of *LMOD2* in schizophrenia because the chromosome 7q31 region includes the *PTPRZ1* (Buxbaum *et al.* 2008) and *FOXP2* (Sanjuán *et al.* 2006) genes that have been indicated to be related to the susceptibility of schizophrenia.

In conclusion, the present findings indicate that PCP can affect the expression of *Lmod2* in an age-dependent, schizophrenomimetic cross-reactive and thalamus-selective manner in mammalian brains (the rat). These figures seem to be consistent with the view that a thalamic neuronal system influenced by PCP may be equipped with a signal pathway containing *Lmod2* or its protein and be functionally

late-developing. Therefore, our PCP data would suggest that changes in *Lmod2* expression should be present in the thalamus of subjects with schizophrenia and a study measuring the expression of that gene in post-mortem CNS is required to confirm this hypothesis.

Acknowledgements

The authors thank Dr Kiyama (Osaka City University) for his generous guidance in DIG- and radioisotope-labelled *in-situ* hybridization techniques and Dr Yoshioka (Teikyo University) for his helpful advice in statistical analyses of the data. This work was partly supported by research grants-in-aid from the Ministry of Health and Welfare, Japan, the Ministry of Education, Culture, Sports, Science and Technology, Japan, and the Social Insurance Agency Contract Fund Commissioned to the Japan Health Sciences Foundation. We received assistance in English editing in the preparation of the present paper by the US Office of the International Technology Exchange Society (an English editing agency) and we are entirely responsible for its scientific content.

AQ6

Statement of Interest

None.

References

Andreasen NC, O'Leary DS, Flaum M, Nopoulos P, Watkins GL, Boles Ponto LL, Hichwa RD (1997). Hypofrontality in schizophrenia: distributed dysfunctional circuits in neuroleptic-naïve patients. *Lancet* **349**, 1730–1734.

Andrews J, Wang L, Csernansky JG, Gado MH, Barch DM (2006). Abnormalities of thalamic activation and cognition in schizophrenia. *American Journal Psychiatry* **163**, 463–469.

Bruneau EG, McCullumsmith RE, Haroutunian V, Davis KL, Meador-Woodruff JH (2005). Increased expression of glutaminase and glutamine synthetase mRNA in the thalamus in schizophrenia. *Schizophrenia Research* **75**, 27–34.

Buchanan RW, Carpenter Jr. WT (2005). Concept of schizophrenia. In: Sadock BJ, Sadock VA (Eds), *Kaplan & Sadock's Comprehensive Textbook of Psychiatry*, 8th edn (pp. 1329–1345). Baltimore: Lippincott Williams & Wilkins.

Buxbaum JD, Georgieva L, Young JJ, Plescia C, Kajiwara Y, Jiang Y, Moskvina V, Norton N, Peirce T, Williams H, *et al.* (2008). Molecular dissection of NRG1-ERBB4 signaling implicates PTPRZ1 as a potential schizophrenia susceptibility gene. *Molecular Psychiatry* **13**, 162–172.

Carlisle HJ, Kennedy MB (2005). Spine architecture and synaptic plasticity. *Trends in Neuroscience* **28**, 182–187.

Clinton SM, Meador-Woodruff JH (2004). Thalamic dysfunction in schizophrenia: neurochemical, neuropathological, and in vivo imaging abnormalities. *Schizophrenia Research* **69**, 237–253.

Conley CA, Fritz-Six KL, Almenar-Queralt A, Fowler VM (2001). Leiomodins: larger members of the tropomodulin (Tmod) gene family. *Genomics* **73**, 127–139.

Dragunow M, Faull RL (1990). MK-801 induces c-fos protein in thalamic and neocortical neurons of rat brain. *Neuroscience Letters* **111**, 39–45.

Duncan GE, Miyamoto S, Leipzig JN, Lieberman JA (1999). Comparison of brain metabolic activity patterns induced by ketamine, MK-801 and amphetamine in rats: support for NMDA receptor involvement in responses to subanesthetic dose of ketamine. *Brain Research* **843**, 171–183.

Dundr M, Ospina JK, Sung MH, John S, Upender M, Ried T, Hager GL, Matera AG (2007). Actin-dependent intranuclear repositioning of an active gene locus in vivo. *Journal Cell Biology* **179**, 1095–1103.

Fischer RS, Fowler VM (2003). Tropomodulins: life at the slow end. *Trends in Cell Biology* **13**, 593–601.

Gouzoulis-Mayfrank E, Heekeren K, Neukirch A, Stoll M, Stock C, Obradovic M, Kovar KA (2005). Psychological effects of (S)-ketamine and N,N-dimethyltryptamine (DMT): a double-blind, cross-over study in healthy volunteers. *Pharmacopsychiatry* **38**, 301–311.

Greifenstein FE, Devault M, Yoshitake J, Gajewski JE (1958). A study of a 1-aryl cyclo hexyl amine for anesthesia. *Anesthesia and Analgesia* **37**, 283–294.

Ibrahim HM, Hogg Jr. AJ, Healy DJ, Haroutunian V, Davis KL, Meador-Woodruff JH (2000). Ionotropic glutamate receptor binding and subunit mRNA expression in thalamic nuclei in schizophrenia. *American Journal Psychiatry* **157**, 1811–1823.

Ito T, Hiraoka S, Kuroda Y, Ishii S, Umino A, Kashiwa A, Yamamoto N, Kurumaji A, Nishikawa T (2007). Effects of schizophrenomimetics on the expression of the CCN1 (CYR 61) gene encoding a matricellular protein in the infant and adult neocortex of the mouse and rat. *International Journal of Neuropsychopharmacology* **10**, 717–725.

Jakary A, Vinogradov S, Feiwell R, Deicken RF (2005). N-acetylaspartate reductions in the mediodorsal and anterior thalamus in men with schizophrenia verified by tissue volume corrected proton MRSI. *Schizophrenia Research* **76**, 173–185.

Javitt DC (2004). Glutamate as a therapeutic target in psychiatric disorders. *Molecular Psychiatry* **9**, 984–997, 979.

Javitt DC, Zukin SR (1991). Recent advances in the phencyclidine model of schizophrenia. *American Journal of Psychiatry* **148**, 1301–1308.

Kaiser S, Foltz LA, George CA, Kirkwood SC, Bemis KG, Lin X, Gelbert LM, Nisenbaum LK (2004). Phencyclidine-induced changes in rat cortical gene expression identified by microarray analysis: implications for schizophrenia. *Neurobiolgy of Disease* **16**, 220–235.

Kong KY, Kedes L (2004). Cytoplasmic nuclear transfer of the actin-capping protein tropomodulin. *Journal of Biological Chemistry* **279**, 30856–30864.

Lahti AC, Weiler MA, Tamara Michaelidis BA, Parwani A, Tamminga CA (2001). Effects of ketamine in normal and schizophrenic volunteers. *Neuropsychopharmacology* **25**, 455–467.

Långsjö JW, Kaisti KK, Aalto S, Hinkka S, Aantaa R, Oikonen V, Sipilä H, Kurki T, Silvanto M, Scheinin H (2003). Effects of subanesthetic doses of ketamine on regional cerebral blood flow, oxygen consumption, and blood volume in humans. *Anesthesiology* **99**, 614–623.

Lisman JE, Coyle JT, Green RW, Javitt DC, Benes FM, Heckers S, Grace AA (2008). Circuit-based framework for understanding neurotransmitter and risk gene interactions in schizophrenia. *Trends in Neuroscience* **31**, 234–242.

MAQC Consortium (2006). The MicroArray Quality Control (MAQC) project shows inter- and intraplatformreproducibility of gene expression measurements. *Nature Biotechnology* **24**, 1151–1161.

McClung CA, Nestler EJ (2003). Regulation of gene expression and cocaine reward by CREB and Delta-FosB. *Nature Neuroscience* **6**, 1208–1215.

Miyasaka M, Domino EF (1968). Neural mechanisms of ketamine-induced anesthesia. *International Journal of Neuropharmacology* **7**, 557–573.

Morgan JI, Curran T (1991). Stimulus-transcription coupling in the nervous system: involvement of inducible proto-oncogenes fos and jun. *Annual Review of Neuroscience* **14**, 421–451.

Nakai K, Horton P (1999). PSORT: a program for detecting sorting signals in proteins and predicting their subcellular localization. *Trends in Biochemical Sciences* **24**, 34–36.

Nagata K, Kiryu-Seo S, Kiyama H (2006). Localization and ontogeny of damage-induced neuronal endopeptidase mRNA-expressing neurons in the rat nervous system. *Neuroscience* **141**, 299–310.

Nishikawa T, Kajii Y, Hiraoka S, Fujiyama K, Sato D, Toda S, Kaneda K, Umino A, Kuroda Y (1998). A molecular pharmacological approach to neural dysfunction in schizophrenia. *Neuroscience Research* (Suppl.) **22**, S8.

Nishikawa T, Umino A, Tanii Y, Hashimoto A, Hata N, Takashima M, Takahashi K, Toru M (1991). Dysfunction of excitatory amino acidergic systems and schizophrenic disorders. In: Nakazawa T (Ed.), *Biological Basis of Schizophrenic Disorders* (pp. 65–76). Tokyo: Japan Scientific Societies Press. Basel: Karger.

Ohba N, Kiryu-Seo S, Maeda M, Muraoka M, Ishii M, Kiyama H (2004). Expression of damage-induced neuronal endopeptidase (DINE) mRNA in peri-infarct cortical and thalamic neurons following middle cerebral artery occlusion. *Journal of Neurochemistry* **91**, 956–964.

Palacios JM, Wamsley JK, Kuhar MJ (1981). High affinity GABA receptors-autoradiographic localization. *Brain Research* **222**, 285–307.

Pérez-Navarro E, Alberch J, Marsal J (1993). Postnatal development of functional dopamine, opioid and tachykinin receptors that regulate acetylcholine release from rat neostriatal slices. Effect of 6-hydroxydopamine lesion. *International Journal of Developmental Neuroscience* **11**, 701–708.

Petersen RC, Stillman RC (1978). *Phencyclidine (PCP) Abuse: An Appraisal.* National Institute on Drug Abuse Research Monograph series, Superintendent of Documents, US Government Printing Office: Washington, DC.

Reich DL, Silvay G (1989). Ketamine: an update on the first twenty-five years of clinical experience. *Canadian Journal of Anaesthesia* **36**, 186–197.

Rose SE, Chalk JB, Janke AL, Strudwick MW, Windus LC, Hannah DE, McGrath JJ, Pantelis C, Wood SJ, Mowry BJ (2006). Evidence of altered prefrontal-thalamic circuitry in schizophrenia: an optimized diffusion MRI study. *Neuroimage* **32**, 16–22.

Sakurai S, Ishii S, Umino A, Shimazu D, Yamamoto N, Nishikawa T (2004). Effects of psychotomimetic and antipsychotic agents on neocortical and striatal concentrations of various amino acids in the rat. *Journal of Neurochemistry* **90**, 1378–1388.

Sanjuán J, Tolosa A, González JC, Aguilar EJ, Pérez-Tur J, Nájera C, Moltó MD, de Frutos R (2006). Association between FOXP2 polymorphisms and schizophrenia with auditory hallucinations. *Psychiatry Genetics* **16**, 67–72.

Sato D, Umino A, Kaneda K, Takigawa M, Nishikawa T (1997). Developmental changes in distribution patterns of phencyclidine-induced c-Fos in rat forebrain. *Neuroscience Letters* **239**, 21–24.

Scalzo FM, Burge LJ (1994). The role of NMDA and sigma systems in the behavioral effects of phencyclidine in preweanling rats. *Neurotoxicology* **15**, 191–200.

Scalzo FM, Holson RR (1992). The ontogeny of behavioral sensitization to phencyclidine. *Neurotoxicology and Teratology* **14**, 7–14.

Schwartz RH, Einhorn A (1986). PCP intoxication in seven young children. *Pediatric Emergency Care* **2**, 238–241.

Segura I, Essmann CL, Weinges S, Acker-Palmer A (2007). Grb4 and GIT1 transduce ephrinB reverse signals modulating spine morphogenesis and synapse formation. *Nature Neuroscience* **10**, 301–310.

Shintomi K (1975). Effects of psychotropic drugs on methamphetamine-induced behavioral excitation in grouped mice. *Europen Journal of Pharmacology* **31**, 195–206.

Shirayama Y, Mitsushio H, Takahashi K, Nishikawa T (2000). Differential effects of haloperidol on phencyclidine-induced reduction in substance P contents in rat brain regions. *Synapse* **35**, 292–299.

Sim K, Cullen T, Ongur D, Heckers S (2006). Testing models of thalamic dysfunction in schizophrenia using neuroimaging. *Journal of Neural Transmission* **113**, 907–928.

Sturgeon RD, Fessler RG, Meltzer HY (1979). Behavioral rating scales for assessing phencyclidine-induced locomotor activity, stereotyped behavior and ataxia in rats. *European Journal of Pharmacology* **59**, 169–179.

Takahashi H, Higuchi M, Suhara T (2006). The role of extrastriatal dopamine D2 receptors in schizophrenia. *Biological Psychiatry* **59**, 919–928.

Tanabe K, Kiryu-Seo S, Nakamura T, Mori N, Tsujino H, Ochi T, Kiyama H (1998). Alternative expression of Shc family members in nerve-injured motoneurons. *Brain Research Molecular Brain Research* **53**, 291–296.

Tanabe K, Nakagomi S, Kiryu-Seo S, Namikawa K, Imai Y, Ochi T, Tohyama M, Kiyama H (1999). Expressed-sequence-tag approach to identify differentially expressed genes following peripheral nerve axotomy. *Brain Research Molecular Brain Research* **64**, 34–40.

Tanii Y, Nishikawa T, Hashimoto A, Takahashi K (1994). Stereoselective antagonism by enantiomers of alanine and serine of phencyclidine-induced hyperactivity, stereotypy and ataxia in the rat. *Journal of Pharmacology and Experimental Therapeutics* **269**, 1040–1048.

Umino A, Takahashi K, Nishikawa T (1998). Characterization of the phencyclidine-induced increase in prefrontal cortical dopamine metabolism in the rat. *British Journal of Pharmacology* **124**, 377–385.

Vollenweider FX, Leenders KL, Oye I, Hell D, Angst J (1997). Differential psychopathology and patterns of cerebral glucose utilization produced by (S)- and (R)-ketamine in healthy volunteers using positron emission tomography (PET). *European Neuropsychopharmacology* **7**, 25–38.

Watis L, Chen SH, Chua HC, Chong SA, Sim K (2008). Glutamatergic abnormalities of the thalamus in schizophrenia: a systematic review. *Journal of Neural Transmission* **115**, 493–511.

Watanabe M, Inoue Y, Sakimura K, Mishina M (1992). Developmental changes in distribution of NMDA receptor channel subunit mRNAs. *Neuroreport* **3**, 1138–1140.

Welch MJ, Correa GA (1980). PCP intoxication in young children and infants. *Clinical Pediatrics (Philadelphia)* **19**, 510–514.

White PF, Way WL, Trevor AJ (1982). Ketamine – its pharmacology and therapeutic uses. *Anesthesiology* **56**, 119–136.